

REPORT

ER-417

TECHNIQUES FOR IMPROVING THE ACCURACY OF NONDISPERSIVE INFRARED-BASED MEASUREMENTS OF COMPLEX MIXTURES OF HYDROCARBONS

Robert D. Stephens
Environmental Research Department

Gregory A. Dorais
University of Michigan

21 October 1994

GM CONFIDENTIAL


DEVELOPMENT CENTER


GM CONFIDENTIAL

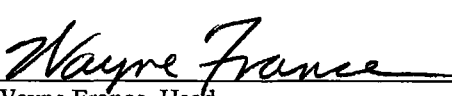
Report No. ER-417

**TECHNIQUES FOR IMPROVING THE ACCURACY
OF NONDISPERSIVE INFRARED-BASED
MEASUREMENTS OF COMPLEX MIXTURES OF
HYDROCARBONS**

21 October 1994

Reported By 
Robert D. Stephens 810-986-1608
Environmental Research Department 8-226-1608


Gregory A. Dorais 313-936-2330
University of Michigan

Approved By 
Wayne France, Head
Environmental Research Department
810-986-1580
FAX: 810-986-1910

Intended Audience: Hughes Santa Barbara Research Center, Powertrain

Technology Area Body, Consumer Sciences, Design, Electronic Systems,
 Environment, Information Technology, Manufacturing, Materials,
 Occupant Information, Powertrain, Safety, Vehicle Systems

**Techniques for Improving the Accuracy of Nondispersive
Infrared-Based Measurements of Complex Mixtures of
Hydrocarbons**

Robert D. Stephens

General Motors Research and Development Center

Gregory A. Dorais

**University of Michigan
Department of Computer Science and Engineering**

Techniques for Improving the Accuracy of Nondispersive Infrared-Based Measurements of Complex Mixtures of Hydrocarbons

Robert D. Stephens and Gregory A. Dorais

Abstract

Simulations of single-channel and multi-channel nondispersive infrared instruments (NDIRs) were performed to identify the optimal number of infrared filters, filter bandwidths, and filter transmission frequencies necessary to provide accurate measurements of complex mixtures of hydrocarbons (HCs). Spectra of 9 individual HC species, 23 vehicle exhaust mixtures, and 4 volatilized-fuel samples along with a reference spectrum containing zero HC were measured. The total HC concentration of each of the HC samples (excluding the reference sample) was also measured via a flame ionization detector (FID). For some analyses, the 37 original spectra were used to generate additional spectra via spectral additions, to yield a total of 703 spectra, each with a known total HC concentration. To create the simulated NDIRs, a number of IR filters with gaussian-shaped filter transmission curves, each with a different bandwidth/transmission frequency combination, were modeled. These simulated IR filters were used with the measured spectra to calculate an absorbance for each spectra using each filter. These absorbances were used in conjunction with FID-measured HC concentrations to perform regression analyses. These analyses identified the filter frequencies, bandwidth, and absorbance coefficients that gave the best predictions of FID-measured HC concentrations.

The optimal NDIR identified by these simulations utilized 13 infrared channels, each with a 20 cm^{-1} bandwidth. Using a test set of 141 HC samples with concentrations ranging from 32.6 to 1101.0 parts-per-million carbon (ppmC), this NDIR had an average absolute error in estimated HC concentration of 6.45 ppmC, where the absolute error of a sample is calculated as the difference between the estimated HC concentration and the FID-measured HC concentration.

Techniques for Improving the Accuracy of Nondispersive Infrared-Based Measurements of Complex Mixtures of Hydrocarbons

Robert D. Stephens and Gregory A. Dorais

Purpose

The purpose of this research was to identify the optimal frequencies, bandwidths, and number of infrared filters that would provide the capability to accurately measure the flame-ionization detector-equivalent total hydrocarbon (HC) concentration in complex hydrocarbon mixtures typical of vehicle exhaust.

Summary

Simulations were performed in which gaussian-shaped transmission curves for infrared filters were used in conjunction with the measured spectral absorbance of a number of different HC samples to predict the absorbances that would be measured if the simulated filters were used in actual NDIR-based instruments. Both single-channel and multi-channel instruments were simulated. The calculated absorbances were used in conjunction with the measured HC concentrations of the samples to determine if the simulated NDIR instruments could accurately measure HC concentrations. The major findings of this work include:

- Single-channel NDIR instruments do not provide the capability to accurately measure the carbon concentrations of complex HC mixtures, but such instruments achieve their best accuracy when utilizing a wide bandwidth (100 cm^{-1}) infrared filter.
- The ability of multi-channel NDIR instruments to measure HC concentrations improves when utilizing infrared filters with narrow bandwidths. The optimal bandwidth identified in this research was 20 cm^{-1} , which yielded the highest accuracy in measuring HC concentrations.
- Simulations of a 13-channel NDIR instrument with 20 cm^{-1} bandwidth yielded an average predicted absolute error of 6.45 parts-per-million carbon (ppmC) when measuring 141 mixtures that had HC concentrations ranging from 32.6 to 1101.0 ppmC. Response factors (i.e. predicted concentration divided by FID-measured concentrations) for these samples had a mean and standard deviation of 0.997 ± 0.046 . This suggests that 95% of all mixtures analyzed could be measured to within 9.2% of the FID-reported HC concentrations using the 13-channel NDIR instrument.

Significance: Design characteristics were identified for a new-generation multi-channel NDIR instrument that would be capable of making accurate measurements of the total HC concentrations in vehicle exhaust mixtures. This technology can be applied to remote emissions sensors to accurately measure the real-world emissions from the on-road vehicle fleet, and/or to identify individual vehicles that are excessive emitters of HC.

Introduction

Nondispersive infrared analyzers (NDIRs) and flame ionization detectors (FIDs) have been used for many years to measure the concentrations of total hydrocarbons (HCs) in vehicle exhaust¹. The limitations of these techniques have also been clearly defined¹. For FID measurements, errors occur when oxygen or oxygen-containing compounds are present. However, if the oxygen and/or oxygenated compound concentrations are known, this interference can be corrected, making FID a highly accurate counter of total carbon atoms present within a sample. For NDIR, measurement accuracy for complex mixtures is highly variable, and changes as a function of the HC species present in the mixture^{1,2}. This is a direct result of the fact that each HC species has a unique infrared absorption strength at any given infrared wavelength. Hence, it is probable that improved NDIR accuracy will require an instrument capable of measuring infrared absorption in a number of different infrared wavelengths.

FIDs are used to measure total HCs emitted during the Federal Test Procedure (FTP) and during IM240 testing. The FTP is utilized to certify new production vehicles to assure that exhaust and evaporative emissions meet new car emissions standards. The IM240 is EPA's recommended Inspection and Maintenance (I/M) test which is used to verify that in-use vehicles are not excessive emitters of HCs, carbon monoxide (CO), and/or oxides of nitrogen (NO_x). NDIRs are still used in a number of state operated I/M programs, however. NDIR is also the technique employed by remote sensing devices (RSDs), which are currently under evaluation as a means to measure the vehicle fleet emissions inventory and/or to enhance existing I/M programs. It is unlikely that an FID-based technique could be employed to remotely measure the HC emissions from on-road vehicles. For this application, infrared techniques have a distinct advantage due to the ability to project an infrared beam through the exhaust of on-road vehicles.

Table I lists the relative accuracy of a commercial NDIR¹ and a RSD² for measuring a number of individual HC species. For all samples listed in this table, the instruments were calibrated with propane.

Hydrocarbon	Non-RSD NDIR	RSD NDIR
Methane	0.30	0.26
Propane	1.00	1.00
n-Butane	1.04	0.99
Ethylene	0.09	0.08
Propene	0.30	0.29
Toluene	0.12	0.07

Motor vehicles emit these and more than 100 other HC species. NDIR will measure each of the many different HC species in vehicle exhaust with a different accuracy. The fact that these accuracies are so variable and, in some cases very low, strongly suggests that

existing NDIRs are not capable of accurately measuring the HC emissions inventory from the vehicle fleet. An NDIR capable of accurately measuring HC concentrations would be a potentially important tool for measuring the HC emissions from the in-use vehicle fleet.

In this work, we utilized FID and infrared spectral measurements to determine the theoretical accuracy of a number of NDIR-based measurement techniques. No instruments were built or tested in this process. Instead, the spectra and FID measurements were used to perform simulations of “theoretical instruments”. That is, we defined instrument characteristics (e.g. transmittance versus wavelength for each infrared channel) and performed simulations to predict the instrument response to many different HC samples.

In this analysis, we evaluated the accuracy, relative to FID, for NDIR measurements that utilized (1) a single channel (i.e., one wavelength range with a defined infrared bandwidth, and (2) multi-channel capability (up to a maximum of 37 infrared channels). In the single-channel NDIR simulations, the impact of changing the bandwidth and filter center frequency of the single channel was explored. For the multi-channel NDIR simulations, selected filter center frequencies were used in some cases, and in other cases, regression analyses were used to identify optimal center frequencies.

These analyses were meant to provide a number of options for instrument designs. Although we have not addressed the issue of instrument costs, these analyses of instrument accuracy should provide instrument design engineers with information needed to determine the cost/accuracy tradeoffs of instruments of various designs.

Experimental

Infrared spectra were measured for 36 samples of HCs using a Nicolet REGA 7000 Fourier Transform Infrared spectrometer operated at 0.5 cm^{-1} resolution. Each of the spectra were carefully baseline corrected prior to our analysis. The samples consisted of 23 automobile exhaust gas samples, 4 volatilized-gasoline samples, 9 different individual HC species that are typically major constituents of automobile exhaust, and a reference sample with zero HC. The exhaust gas samples were generated by vehicles operated on dynamometers located at either GM R&D² or California Air Resources Board³ (CARB). At GM, the exhaust samples were collected undiluted and were partially dehumidified by cold traps, whereas at CARB the samples were collected from constant volume samplers and were not dehumidified. The total HC concentration of each sample, except the reference sample, was also measured via FID. **Table II** lists the mean concentrations in parts-per-million of carbon and the concentration ranges present in the various samples included in these analyses. The original 36 spectra appear as **Figures A1 through A36** in the appendix.

The infrared transmission that is measured via an NDIR for any given HC sample is a function of the transmission through both the sample and the infrared filter used by the NDIR. The theoretical filter transmission curves (T_f) utilized for this work were generated by the following equation:

$$T_f(i) = e^{-(4 \log(2)(i-c)^2 w^{-2})} \quad (1)$$

Table II Carbon Concentrations of HC Samples

Sample	# Samples	Mean Conc. (ppmC)	Min. Conc. (ppmC)	Max. Conc. (ppmC)
GM Exhaust	12	374.5	273.6	511.3
GM Individual HCs	9	502.7	87.0	1101.0
GM Volatilized Fuel	4	170.3	104.0	275.2
CARB Exhaust	11	102.8	60.4	157.3

where i is the frequency in wavenumbers (cm^{-1}), c is the center frequency of the filter in wavenumbers, and w is bandwidth in wavenumbers of the filter. The bandwidth was defined as the width of the transmission curve at half of peak transmittance, and the center frequency was defined as the frequency, in wavenumbers, at maximum transmittance.

Using the theoretical filter transmission and the measured transmission (T_s) through each HC mixture, the overall transmission through both the filter and sample (T) was calculated via the following equation:

$$T = \frac{\int_a^b T_f(i) T_s(i) di}{\int_a^b T_f(i) di} \quad (2)$$

where $a=2700 \text{ cm}^{-1}$ and $b=3200 \text{ cm}^{-1}$ were used as the limits of integration for our calculations. Since the transmission through the filter, T_f , approaches 0 outside these limits, the overall transmission, T , outside these limits is negligible and was ignored. Note that the peak percent transmission occurs when $i = c$ in equation (1); i.e., $T_f(c)=1$. Although no physical infrared filter reaches 100% transmission at its center frequency, a maximum transmission parameter multiplied by T_f to reduce peak transmission would cancel out in equation (2). Hence, for simplicity, such a term has not been used.

Since absorbances are additive according to Beer's law, we utilized the original 36 absorbance spectra (and an additional zero absorbance "reference" spectrum to simulate zero HC) to generate an additional 666 spectra ($36 \times 37 \div 2$) by spectral additions of unique combinations of the original 37, yielding a total of 703 samples. This was accomplished by summing 50% of the absorbances that were measured for each of the two unique spectra that were combined. Likewise, HC concentrations for these simulated samples were calculated by summing 50% of the concentrations of the two combined samples.

Theoretical filter transmission curves were calculated via equation (1) for a wide range of infrared filters and used in conjunction with the transmission spectra to calculate the absorbance that would be measured by a simulated NDIR. These absorbances were used in conjunction with FID-measured HC concentrations to perform regression analyses to create linear models that predict the HC concentrations in each of the samples. The extent to which predicted and measured HC concentrations agree is a quantitative measure of the accuracy of the NDIR being simulated.

Results

The NDIR models created to predict HC concentration from the transmission spectra of gas samples were divided into two groups: (1) models using a single filter and (2) models using multiple filters. The results obtained using models from each group are presented in the remainder of this section.

Simulations of Single-Channel NDIRs

The filters were simulated at 361 different center frequencies from 2800 to 3160 cm^{-1} . Simulations were performed for each of these center frequencies using five different bandwidths, for a total of 1805 combinations of filter bandwidth and center frequency. Filter bandwidths tested were 20, 40, 55, 100, and 150 cm^{-1} . The filter bandwidths and center frequencies were varied to assess the relationship between these parameters and the ability of the “simulated” NDIR to predict FID-measured HC concentrations. **Figure 1** shows how the correlation (r^2) values varied with filter center frequency for four of the filter bandwidths, as tested using only the original 36 HC samples. Note that for single filter models, wider bandwidth filters permit more accurate models and have r^2 values that are less sensitive to the filter center frequency.

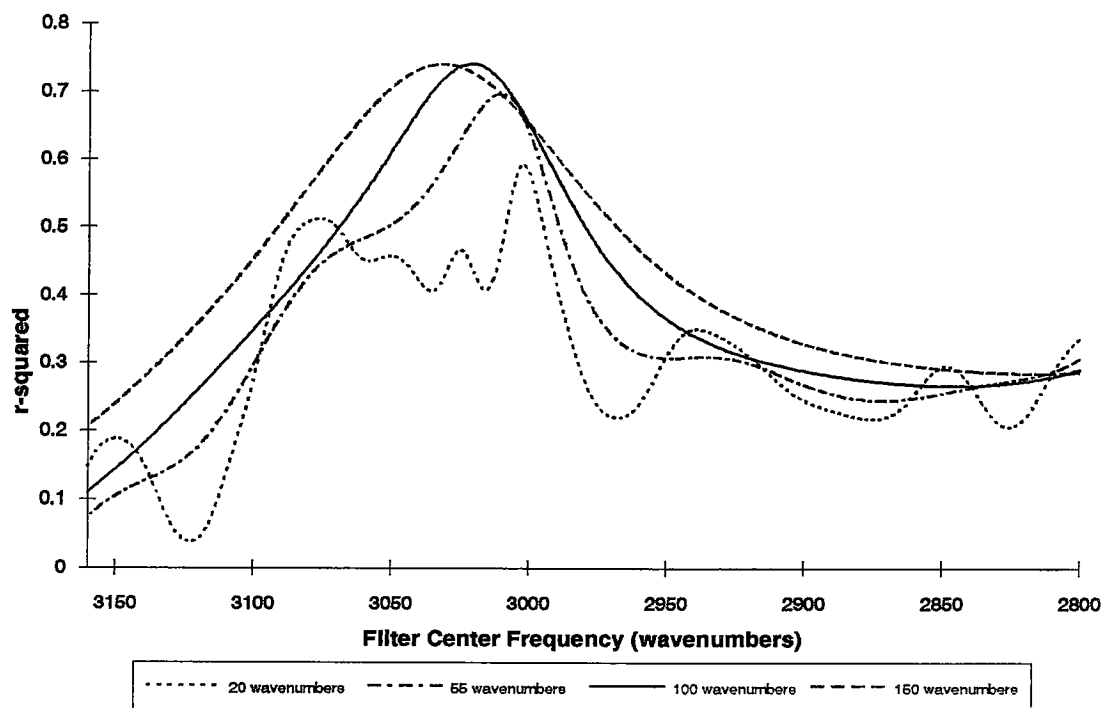


Figure 1. This figure shows how the correlation between predicted and measured HC changes for the original 36 HC samples as a function of center frequency when using four different filter bandwidths.

Of the simulations performed, the best single-channel NDIR has a bandwidth of 100 cm^{-1} and a center frequency of 3021 cm^{-1} . Applying this filter to the entire set of 703 samples yielded a correlation (r^2) between predicted HC and measured HC of 0.747.

We have also calculated the response factors (i.e. the ratio of predicted to measured HC concentrations) for each of the simulated single-channel NDIRs that yielded the best results at any given filter bandpass. The mean and standard deviation of the response factors obtained for the 703 complex HC mixtures are listed in Table III. A plot of the predicted HC concentration obtained by the 100 cm^{-1} bandwidth model as a function of the FID-measured HC concentration is shown as Figure 2.

Filter Bandwidth (cm^{-1})	Center Frequency (cm^{-1})	r²	Response Factor Mean	Response Factor Std. Dev.
20	3002	0.609	1.193	0.532
40	3005	0.665	1.138	0.433
55	3010	0.707	1.116	0.410
80	3017	0.740	1.101	0.397
100	3021	0.747	1.096	0.397
150	3032	0.745	1.096	0.419

Simulations of Multiple-channel NDIRs

Linear models of NDIRs using multiple channels were also developed. The first model used five filters each with a bandwidth of 55 cm^{-1} , which is a typical width of available narrow band optical filters. A filter of this bandwidth is currently used by a remote sensor designed at GM R&D¹. The filter center frequencies were selected as 2879 cm^{-1} , 2925 cm^{-1} , 2962 cm^{-1} , 3009 cm^{-1} , and 3084 cm^{-1} which correspond to frequencies near the bandcenters of C-H bond types⁴ of compounds that are major components of vehicle exhaust. The infrared absorbance for each of these filters was calculated for each of the original 36 HC samples. Multiple regression was then used to calculate the coefficients and y-intercepts that yield predicted HC concentrations that best agree with the actual HC concentration of each sample. The multiple correlation (r^2) between predicted and measured HC concentration for the 703 samples was 0.889 with a response factor mean of 1.082 ± 0.331 , where the uncertainty value represents one standard deviation.

Four additional multi-channel models were then developed, each using a different, but constant, filter bandwidth. Bandwidths studied included 20, 40, 60 and 100 cm^{-1} . Filters with bandwidths less than 20 cm^{-1} were not examined because of the difficulties involved in physically making such filters. In the development of each model, absorbances for the 703 samples were calculated for each of 37 different filters.

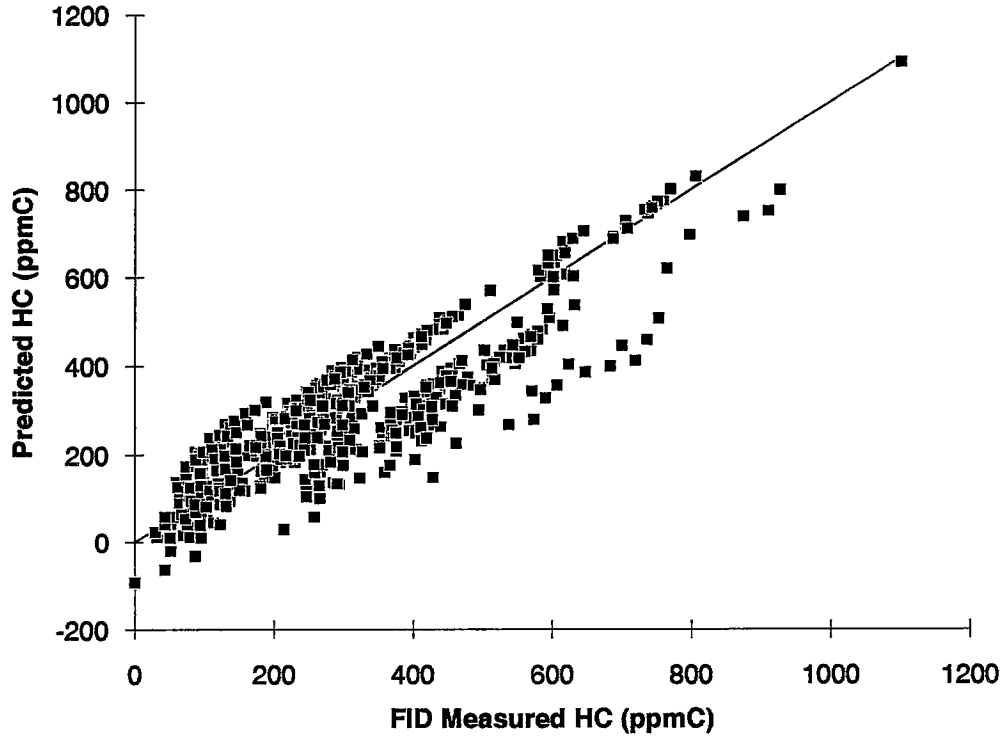


Figure 2. *This figure shows the predicted HC concentrations derived from the 100 cm^{-1} bandwidth single-channel NDIR model versus the FID-measured HC concentration. The solid line represents a perfect correlation between predictions and measurements.*

These absorbances were used in conjunction with the measured HC concentrations as inputs to a regression model. The filters had peak transmittances spaced at equal increments of 10 cm^{-1} from 2800 to 3160 cm^{-1} . Although it would be possible for each model to use all 37 filters, step-wise multiple regression with manual optimization was used to select both the quantity of filters and the optimal center frequencies of the filters for each model. In many cases, filter overlap limited the number of unique filters used in the models, since the absorbances calculated for adjacent channels were sometimes highly correlated. As the bandwidth increased, the correlation between absorbances in adjacent channels increased.

The regression model created for each filter bandwidth identified a different number of filters required to accurately predict FID-measured HC concentrations. Not surprisingly, each model had differing accuracy in the HC predictions. A plot of the mean of the absolute residual HC values obtained for each of the four models is shown in **Figure 3**, where the residual HC values are the FID-measured ppmC minus the predicted ppmC values.

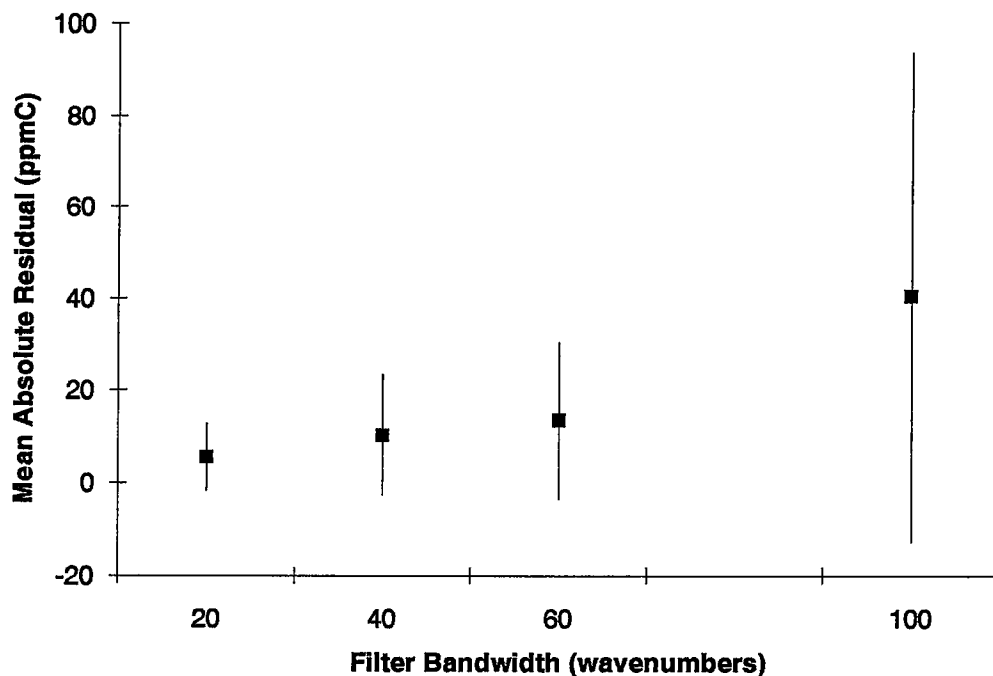


Figure 3. This figure shows the mean of the absolute values of the residuals (measured HC minus predicted HC in ppmC) from the four models generated using different filter bandwidths. The error bars indicate ± 1 SD.

The most accurate model used a filter bandwidth of 20 cm^{-1} and used 13 channels. Using this model with all 703 samples, the mean of the absolute values of the residuals was 5.9 ppmC and the standard deviation of the residuals was 7.7 ppmC. This residual represents a 2.0% error of the mean HC concentration (292.7 ppmC) of the 703 HC samples. The response factors and residual values obtained for the four models are summarized in Table IV.

Filter Bandwidth	# Channels	r^2	Mean Abs. Residual HC ppmC	Residual HC Std. Dev. ppmC	Mean R. F.	R. F. Std. Dev.
20	13	0.998	5.85	7.72	1.002	0.040
40	11	0.993	10.7	13.6	1.008	0.095
60	9	0.989	13.8	17.4	1.016	0.111
100	7	0.881	43.4	57.7	1.066	0.323

From the above table, we see that the response factor standard deviations increase significantly, from 0.040 to 0.323 as the filter bandwidths increase from 20 to 100 cm^{-1} .

Figures 4 and 5 show the placement of the filters along the spectrum for the 40 cm^{-1} bandwidth model and the 20 cm^{-1} bandwidth model, respectively.

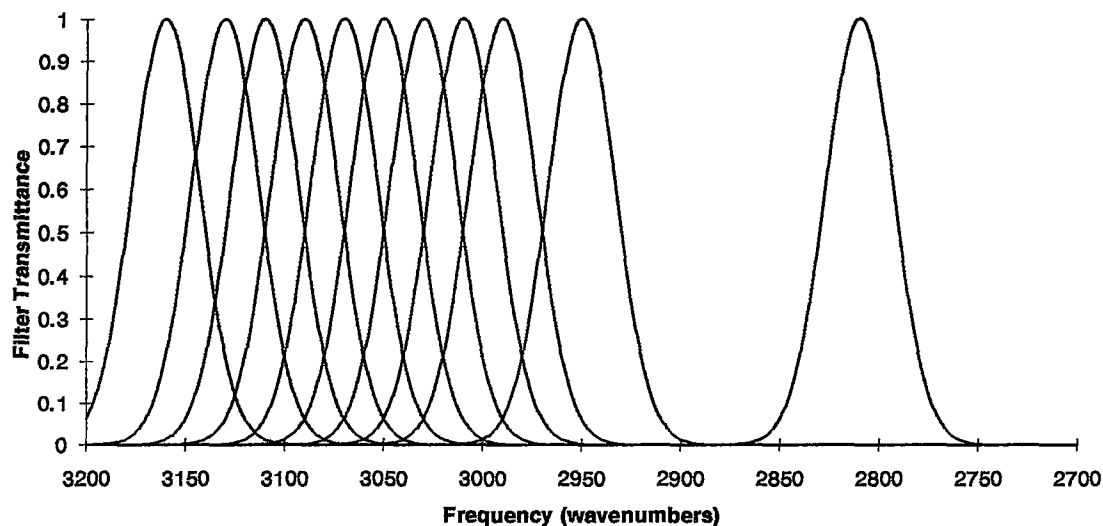


Figure 4. This figure shows the optimal filter frequencies obtained by the 40 cm^{-1} bandwidth simulation.

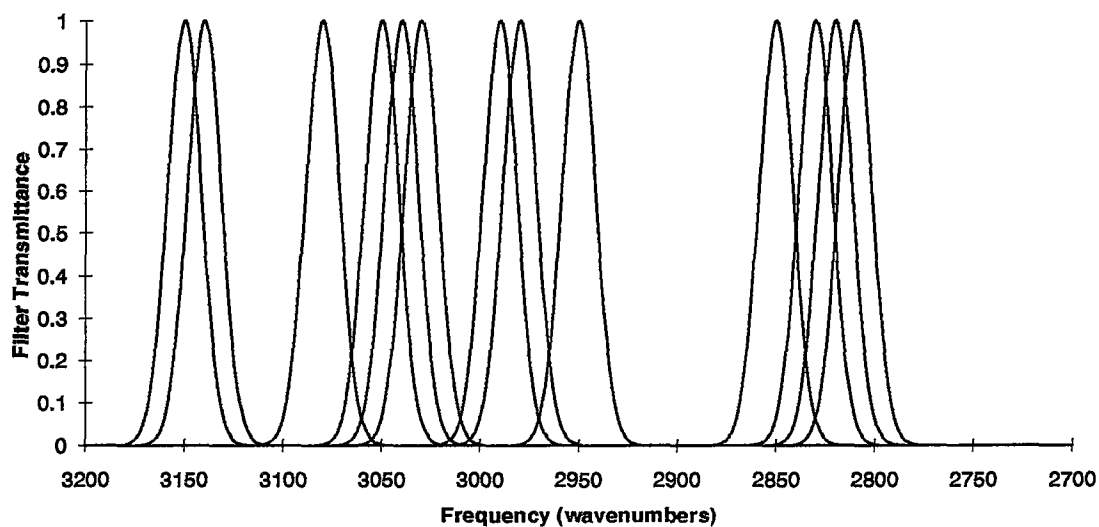


Figure 5. This figure shows the optimal filter frequencies obtained by the 20 cm^{-1} simulation.

The similarities in center frequencies identified by the two models suggest that the various HC samples can be distinguished from one another by the absorbance features present at these frequencies.

Filter Center Freq. (cm⁻¹)	Model Coefficient (703 Samples)	Mean Coefficient^a (562 Samples)	Std. Dev. Coefficient^a (562 Samples)
2810	-58,114	-58,205	1,242.8
2820	91,122	91,226	801.2
2830	-43,271	-43,317	476.9
2850	4,381	4,383	133.1
2950	1,192	1,193	16.4
2980	-1,167	-1,169	22.0
2990	637	640	27.4
3030	-726	-732	39.0
3040	8,017	7,997	268.3
3050	-11,693	-11,662	310.0
3080	8,817	8,813	71.4
3140	-21,990	-21,979	85.9
3150	25,929	25,914	84.1
	4.3 ^b	4.3 ^b	0.7 ^b

^a Five sets of HC samples were used, each of which consisted of 562 samples that were randomly selected from the original 703 samples.

^b This is the value of the constant in the regression equation, which takes the following form:

$$HC(\text{predicted}) = a(A_{\nu 1}) + b(A_{\nu 2}) + c(A_{\nu 3}) \dots + \text{constant}$$

where *a*, *b*, and *c* are the coefficients and $A_{\nu i}$ are the absorbances at each filter wavelength.

For the 20 cm⁻¹ bandwidth model, it is noteworthy that adjacent filters have dramatically different regression coefficients, as listed in Table V. Filters with center frequencies close together usually have absorbances that are highly correlated. However, closely adjacent filters are sometimes used by the model, typically resulting in coefficients of opposite sign and large, but nearly equal magnitude. For example, in the above table we see the closely adjacent filters with centers at 2810, 2820, and 2830 cm⁻¹ have coefficients that vary dramatically from -58,114.21 to +91,121.70 then back to -43,271.28, respectively. The same phenomenon occurs with the filters at 3140 and 3150 cm⁻¹. As the number of filters in the models increase, the accuracy of the predicted HC concentrations increase. However, the frequency of large-magnitude changes in coefficients also increases.

These large variations in the coefficients suggests that the model is highly sensitive to the inputs. For example, if different HC samples were used in the analysis, it is possible that dramatically different regression coefficients would be obtained. To test this possibility, the step-wise multiple regression analyses were repeated using five different randomly selected subsets that consisted of 80% of the original 703 samples. Each stepwise regression was repeated for each of these five sample inputs at each bandwidth. Each of the five different bandwidth models were then evaluated using the

five different sets of the remaining 20% of the original 703 samples. In this way, the variability of the regression coefficients could be determined as a function of different HC sample inputs. Also, the ability of the models to predict HC concentrations in samples not used as inputs could be tested by using the remaining 20% of the samples.

In Table V, we have listed the magnitude of the swings in the regression coefficients obtained from the five different sets of HC sample inputs used in the 20 cm^{-1} bandwidth simulation. The response-factor means of the five sets of HC samples not included in the model creation ranged from 0.997 to 1.009 with a mean of 1.003. The response-factor standard deviations for the same samples ranged from 0.038 to 0.046, suggesting that even the worst-case test set yields an error of no greater than 9.2% (0.046×2) for 95% of the measurements. Using this “worse-case” test set as an example, we have plotted the predicted HC concentration versus the FID-measured HC concentration in Figure 6.

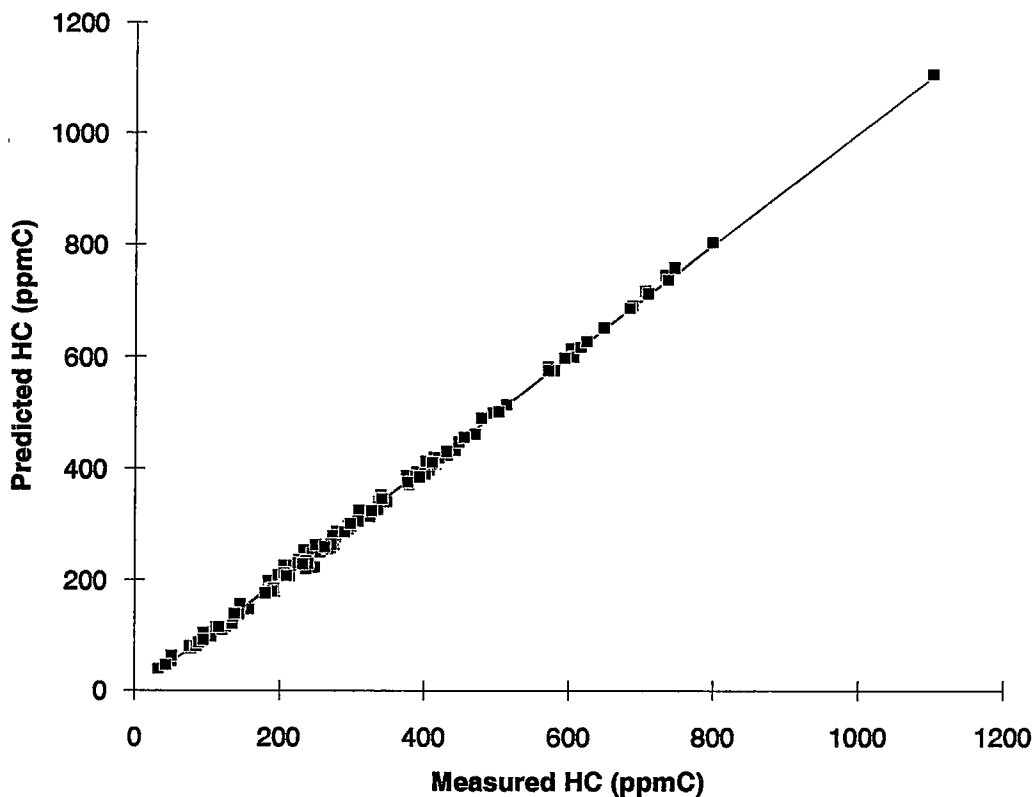


Figure 6. This figure shows a plot of the predicted versus measured HC of the 141 test samples from the test set with the poorest fit (standard deviation of R.F. = 0.046). The predicted concentrations were derived from the 20 cm^{-1} bandwidth NDIR model created from the other 562 of the original 703 samples. The solid line represents a perfect correlation between measurements and predictions.

Discussion

NDIRs capable of accurately measuring the carbon concentrations in complex mixtures of HCs would be useful in I/M applications that utilize either remote sensors or instruments located at fixed site test stations. The simulations described in this report indicate that multi-channel NDIRs are capable of providing accurate measurements if filter bandwidths and transmission characteristics are chosen carefully.

Narrow band optical filter technology has progressed to the point that it is possible to create filters in which the transmission wavelengths vary as a function of position along a linear axis of the filter. Such “wedge” filters mounted on a detector array make it possible to create relatively inexpensive multi-channel NDIR spectrometers. The multi-channel NDIRs modeled in this report are analogous to instruments that could be built using this technology.

However, there are considerations that are important to the implementation of the NDIRs described in this report. For example, the large regression coefficients obtained by these simulations might pose a problem for experimental measurements. Such an instrument might have high sensitivity to noise present in the channels that have large positive or negative regression coefficients. Should this become a problem, it appears that instrument accuracy might actually increase if fewer filters with wider bandwidths were used, since this would minimize the large coefficient swings. Also, the accuracy of such an instrument is a function of the number and diversity of HC samples used as inputs in the regression model. Although we have tested our models on five different data sets, each containing between 139 and 141 different HC mixtures (20% of 703), it is possible that larger errors than we report would result from measurements performed on mixtures that are dramatically different than ours. However, our modeling was performed on HC samples with widely differing concentrations of alkanes, alkenes, alkynes and aromatics. Therefore, we believe that good results (low HC residuals and response factors consistently near one) will be possible on other HC mixtures, although it might be necessary to recompute optimal filter characteristics and regression coefficients.

NDIR systems based upon filters with variable bandwidths are also possible, but have not been explored in these analyses. The similarities in center frequencies chosen by the 20 cm^{-1} and 40 cm^{-1} models suggest that the various HC samples can be distinguished from one another by absorption features present within the bandwidth of these filters. Hence, it may also be possible to use a system with variable bandwidth filters to take advantage of the overlap that occurs in the bandwidths of the 20 cm^{-1} filters. For example, an effective system might utilize 40 cm^{-1} bandwidth filters centered at 2820 cm^{-1} and 3040 cm^{-1} , 30 cm^{-1} filters centered at 2985 cm^{-1} and 3145 cm^{-1} , and 20 cm^{-1} bandwidth filters centered at 2850 cm^{-1} , 2950 cm^{-1} , and 3080 cm^{-1} . Such a system would utilize all of the spectral regions utilized by the 20 cm^{-1} bandwidth system, but have the potential advantage of increased signal-to-noise ratio in the wider bandwidth channels.

Another consideration relevant to the implementation of multi-channel NDIRs is the potential for water interference. Infrared absorption by water vapor does occur in the same spectral region as HCs. In the exhaust samples used in this study, water vapor concentrations were unknown. However, the relative humidity of the various GM exhaust samples were probably relatively constant due to similar sample preparations (i.e. all GM exhaust samples were collected after cold traps to limit the water vapor

concentration). The CARB exhaust samples were not pre-treated to remove or decrease the water vapor content. The nine individual HC samples were prepared from cylinder gases; hence, water vapor concentrations were probably negligible in these samples.

The magnitude of the potential impact of the water interference is difficult to quantify. However, for the 20 cm^{-1} bandwidth analysis, large HC errors were not observed despite the large variability that probably exists in the water vapor concentrations of the various samples. This suggests that the water interference is small. Alternatively, it is possible that the regression analysis has been successful at determining coefficients that have removed this potential interference.

To the extent that water vapor is an interference, the importance of this interference will depend upon the particular NDIR application. For an NDIR that can use sample preparation, e.g. pumping a sample through a chilled water condensation trap, the water interference can be limited to some extent, by decreasing the water concentration. For remote sensing applications, the magnitude of the interference will depend partially upon the ambient relative humidity. This is because with the infrared pathlengths typically used for cross-road remote sensing, some of the water absorption lines will probably be totally absorbing at high humidity, hence additional water vapor in vehicle exhaust will not contribute any additional infrared absorption at these wavelengths. At low relative humidity, fewer lines will be totally absorbing, and, for those lines not totally absorbing, additional infrared absorption would occur due to water vapor in vehicle exhaust.

Conclusions

Previous research has indicated that currently available single-channel NDIRs are not capable of accurately measuring the HC concentrations of complex HC mixtures. These simulations indicate that there is no single filter combination of center frequency and bandwidth that provides accurate measurements of the concentration of complex HC mixtures. However, the accuracy of single-filter NDIRs does increase as the bandwidth of the filter increases.

These simulations indicate that it is possible to accurately measure the carbon concentrations of complex HC mixtures when using multi-channel NDIRs. The simulations indicate that multi-channel NDIR accuracy improves as the filter bandwidth decreases.

The simulated NDIR that yielded the best agreement with FID measurements was a 13-channel, 20 cm^{-1} bandwidth system. This model was tested on 141 complex mixtures of HCs with concentrations that ranged from 0 to 1101 ppmC. For these samples, the largest error in predicted HC for the 20 cm^{-1} bandwidth NDIR, was 36.4 ppmC. Response factors (i.e. predicted concentration divided by FID-measured concentrations) for these samples had a mean and standard deviation of 0.997 ± 0.046 . This suggests that 95% of all mixtures analyzed could be measured to within 9.2% of the FID-reported concentrations.

Acknowledgments

The authors wish to thank Paul Rieger and John Kuhlberg of the California Air Resources Board and Pat Mulawa of GM for providing the infrared spectra and FID data utilized in these analyses.

References

1. Jackson, M. W., "Analysis for Exhaust Gas Hydrocarbons: Nondispersive Infrared versus Flame-Ionization", *J. Air Poll. Cont. Assoc.*, 11 697 (1966).
2. Stephens, R. D., Mulawa, P. A., Giles, M. T., Kennedy, K. G., Groblicki, P. J., Cadle, S. H., Duncan, J. W., Knapp, K. T., "An Experimental Evaluation of the Accuracy of Remote Sensor Measurements of Hydrocarbons", CRC-APRAC Contract VE-11-4 Final Report, September, 1994.
3. Rieger, P. and Kuhlberg, J., California Air Resources Board, Haagen-Smit Laboratory, 9528 Telstar Ave., El Monte, CA, 91731, Private Communication, June 22, 1994.
4. Sverdlov, L. M., Kovner, M. A., Krainov, E. P., Vibrational Spectra of Polyatomic Molecules, John Wiley and Sons, Inc. New York, NY, 1974.

Appendix

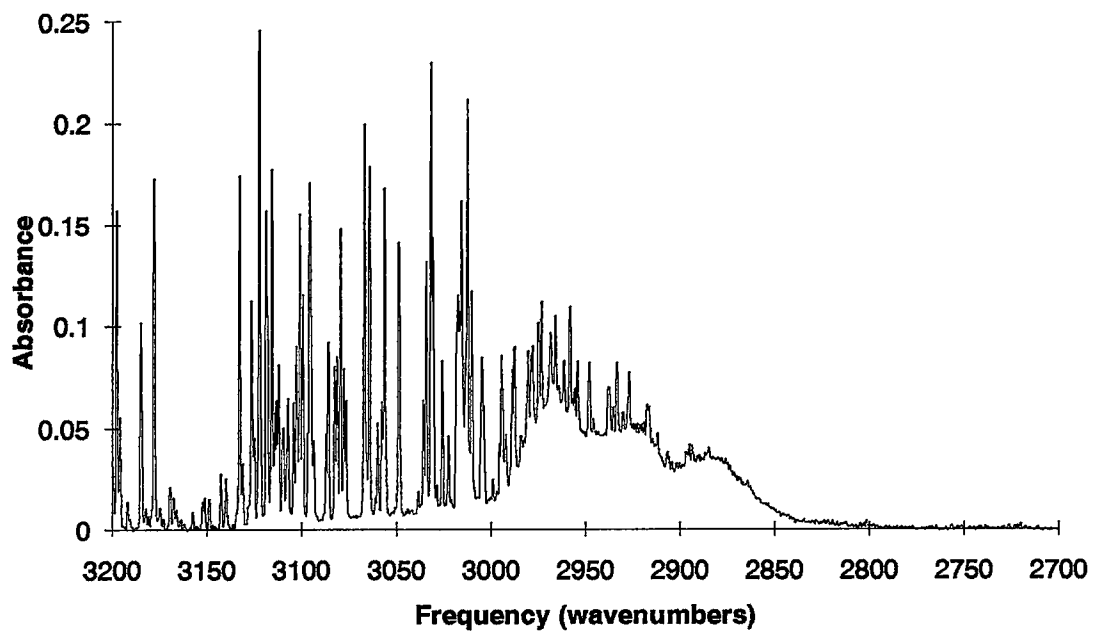


Figure A1. Spectrum of CARB exhaust sample 10BA3³ with measured HC of 65.1 ppmC.

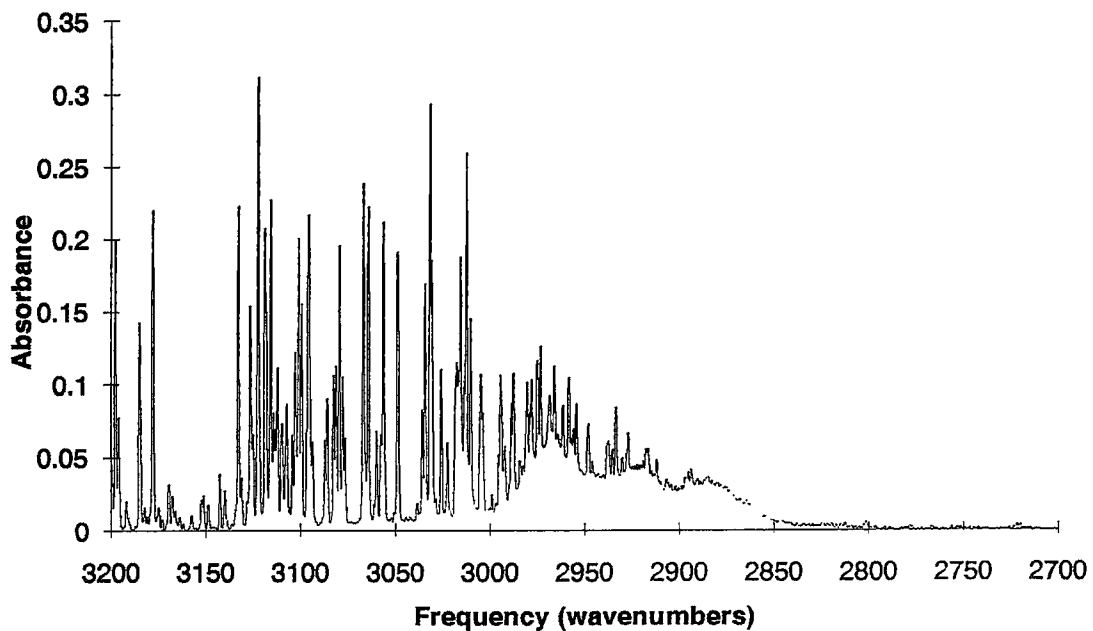


Figure A2. Spectrum of CARB exhaust sample 20BA5³ with measured HC of 60.4 ppmC.

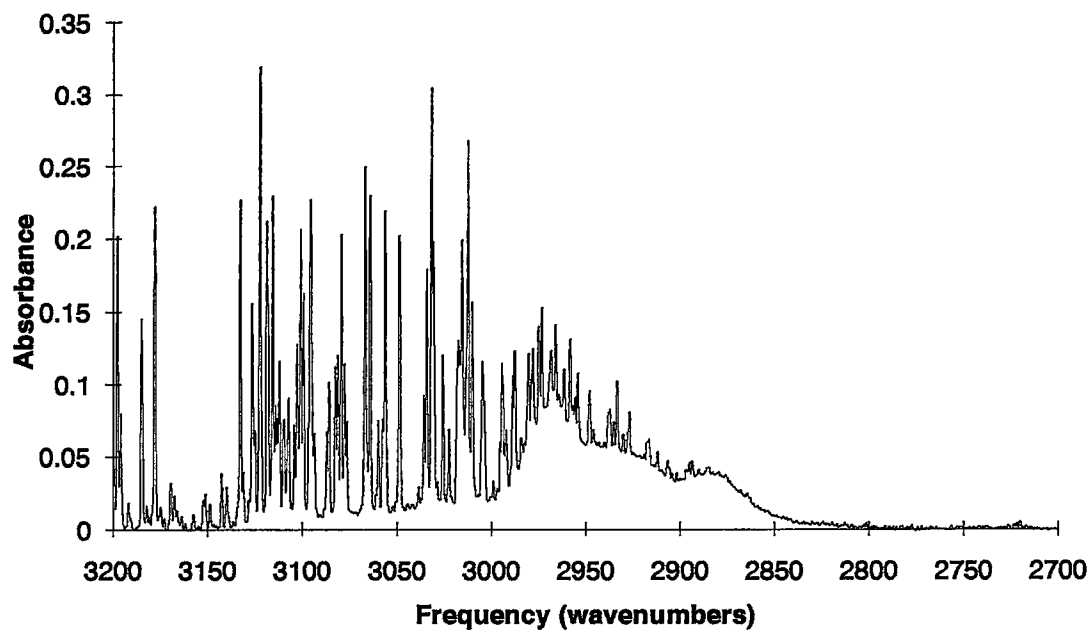


Figure A3. *Spectrum of CARB exhaust sample 23BA4³ with measured HC of 100.6 ppmC.*

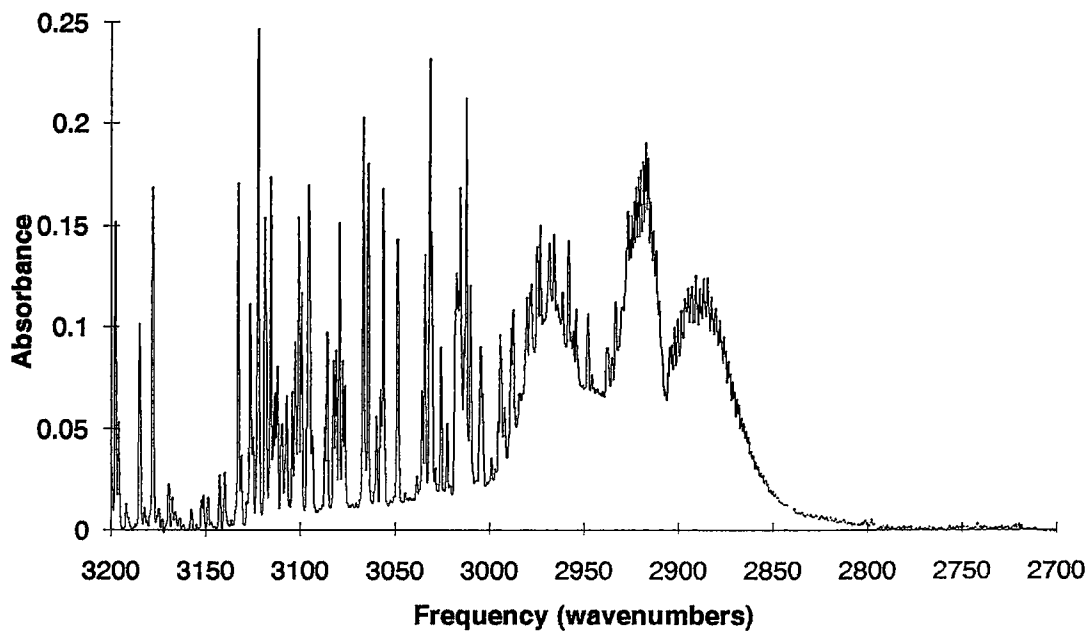


Figure A4. *Spectrum of CARB exhaust sample 27BA3³ with measured HC of 103.9 ppmC.*

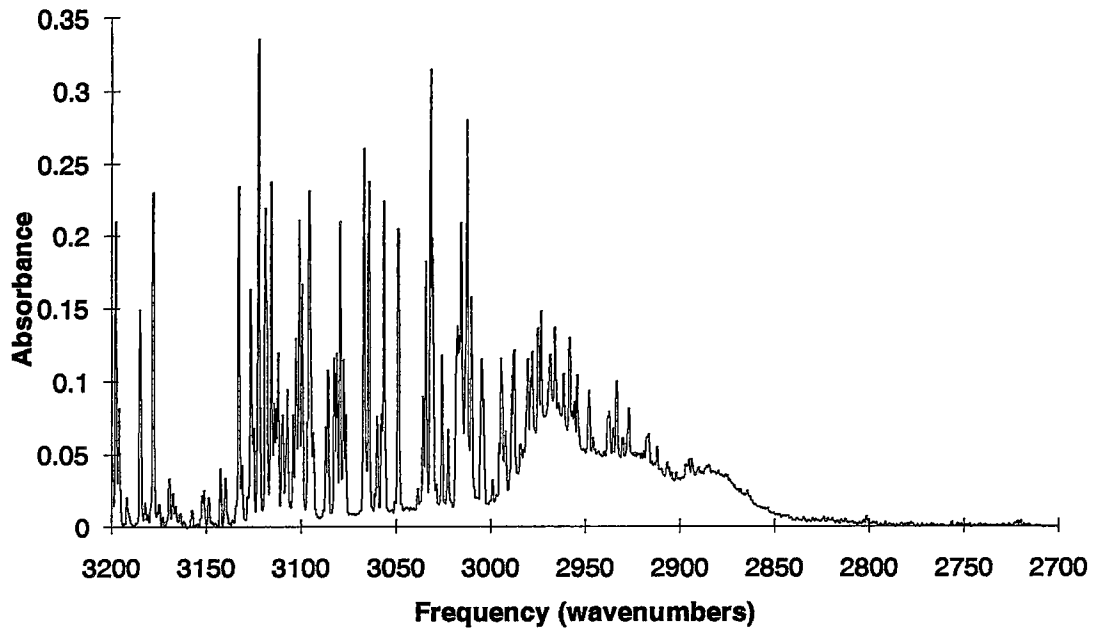


Figure A5. *Spectrum of CARB exhaust sample 32BA3³ with measured HC of 90.1 ppmC.*

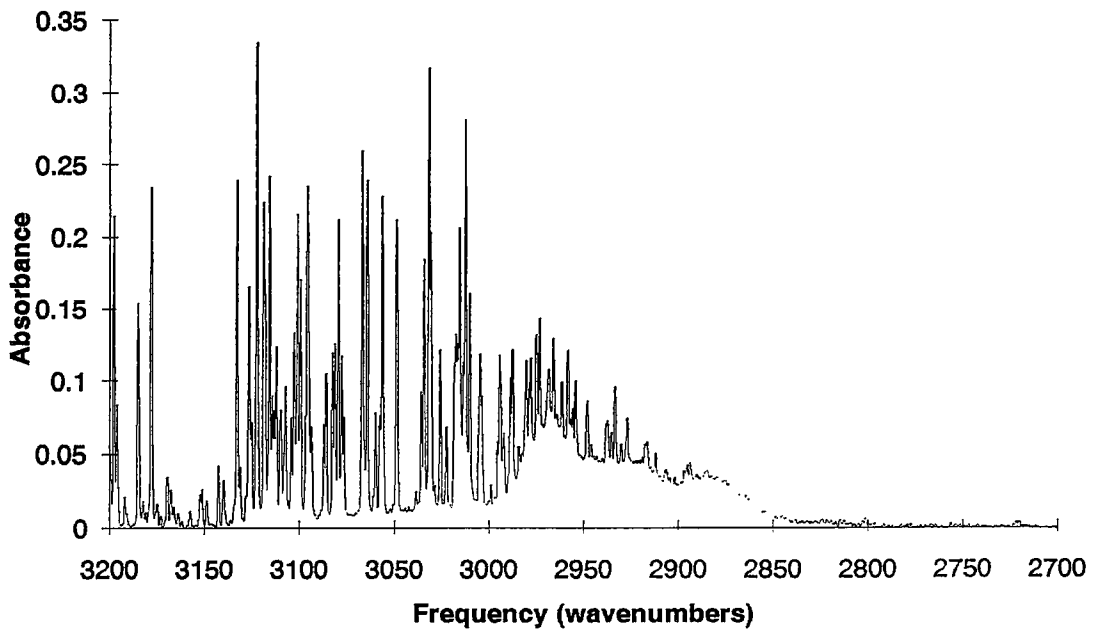


Figure A6. *Spectrum of CARB exhaust sample 32BA4³ with measured HC of 88.3 ppmC.*

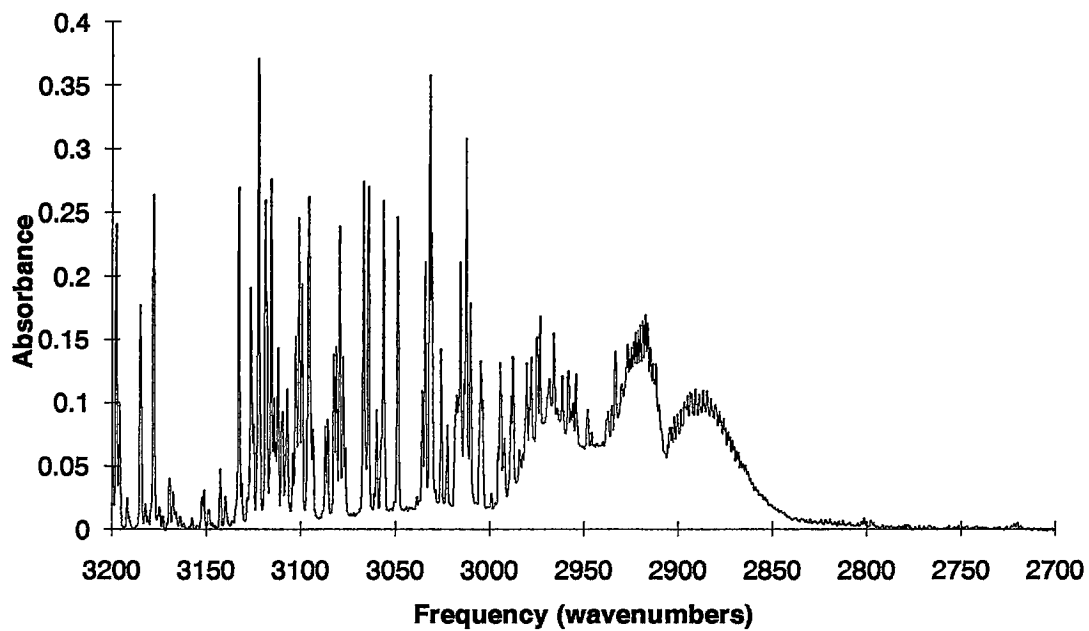


Figure A7. *Spectrum of CARB exhaust sample 4BA4³ with measured HC of 111.3 ppmC.*

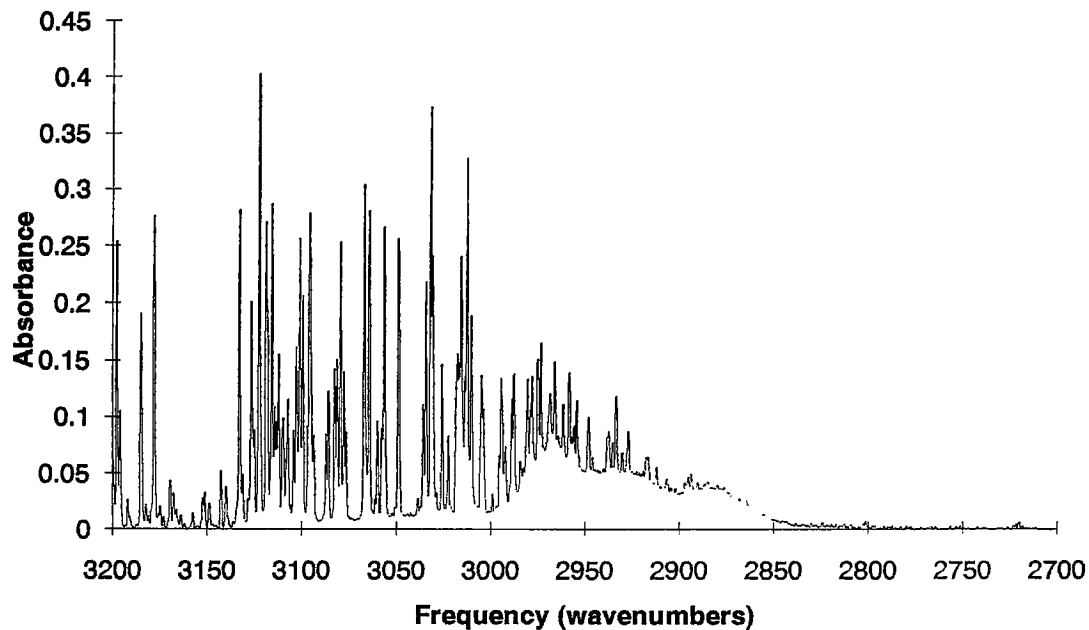


Figure A8. *Spectrum of CARB exhaust sample 6BA4³ with measured HC of 87.4 ppmC.*

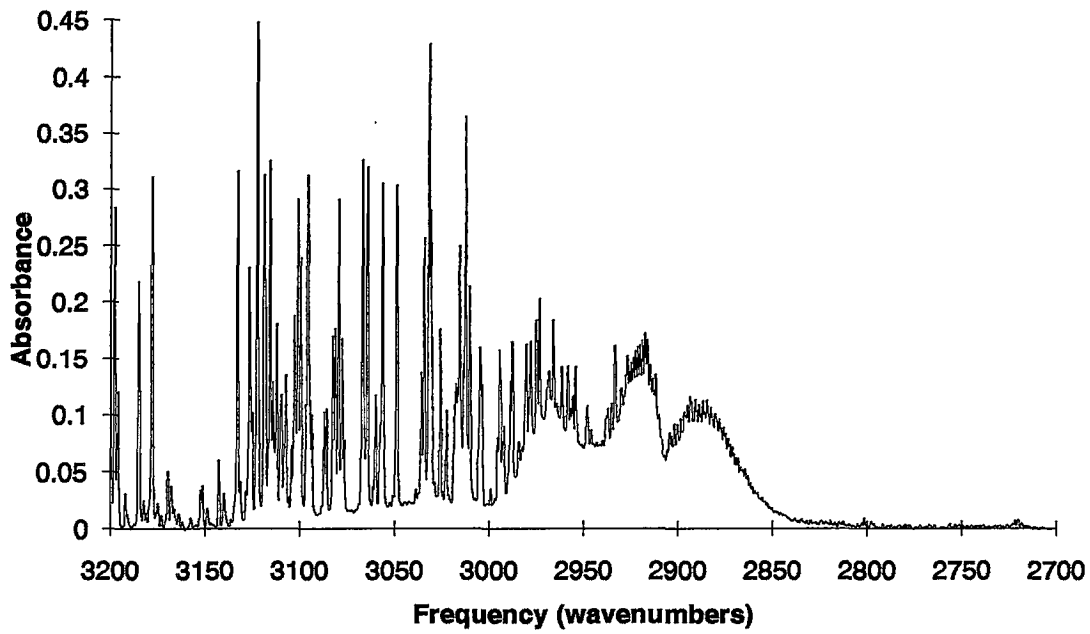


Figure A9. *Spectrum of CARB exhaust sample 7BA5³ with measured HC of 130.4 ppmC.*

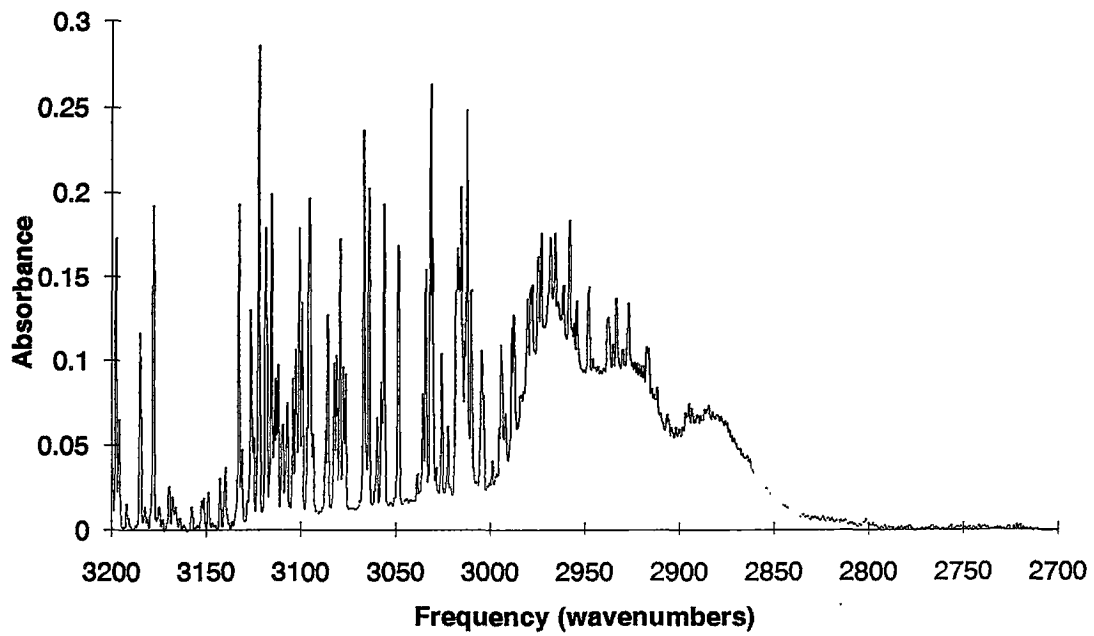


Figure A10. *Spectrum of CARB exhaust sample 8BA3³ with measured HC of 135.9 ppmC.*

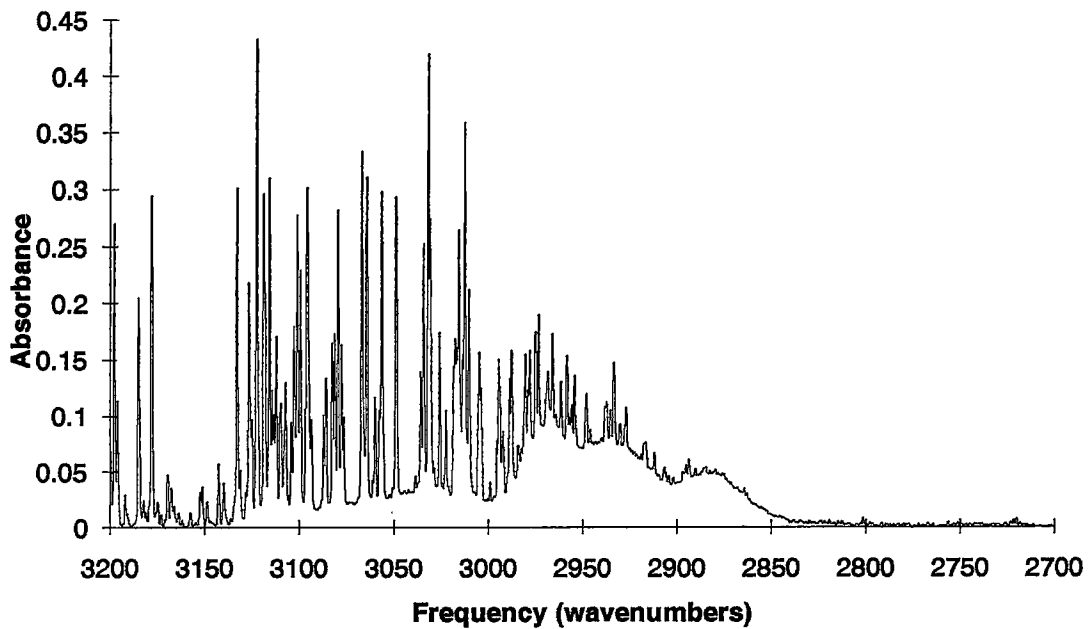


Figure A11. *Spectrum of CARB exhaust sample 9BA3³ with measured HC of 157.3 ppmC.*

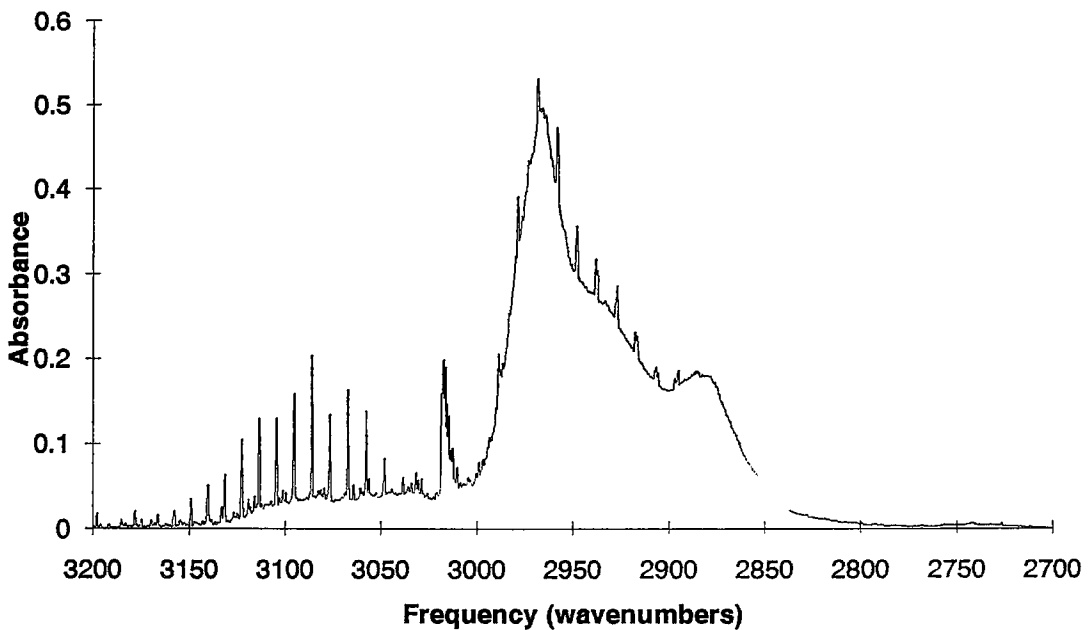


Figure A12. *Spectrum of GM exhaust sample A52601B² with measured HC of 374.3 ppmC.*

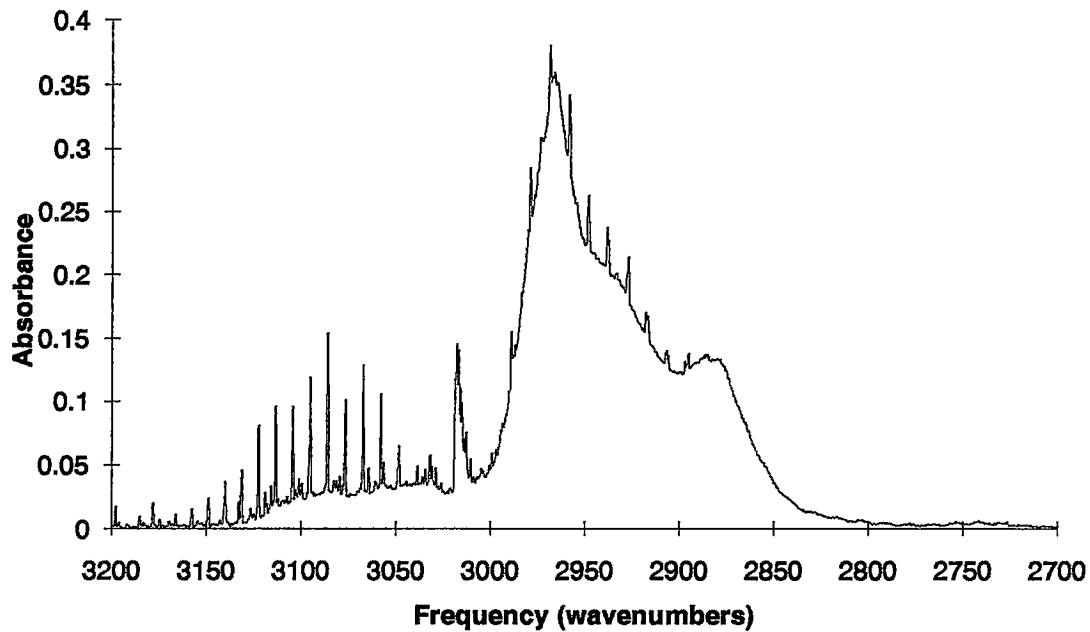


Figure A13. *Spectrum of GM exhaust sample A52802A² with measured HC of 273.7 ppmC.*

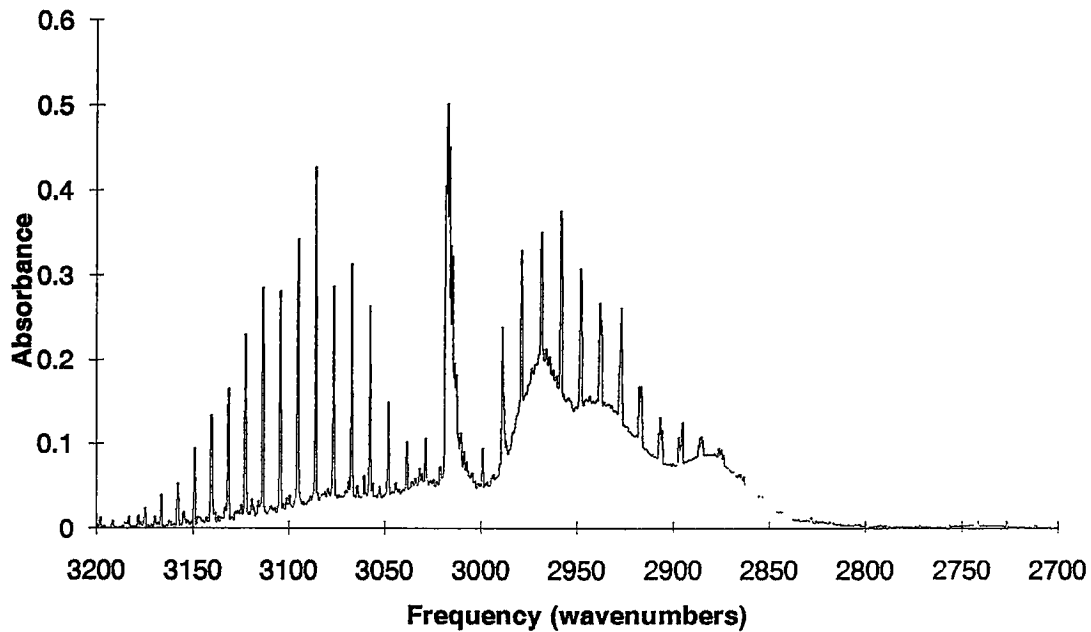


Figure A14. *Spectrum of GM exhaust sample A60101A² with measured HC of 309.1 ppmC.*

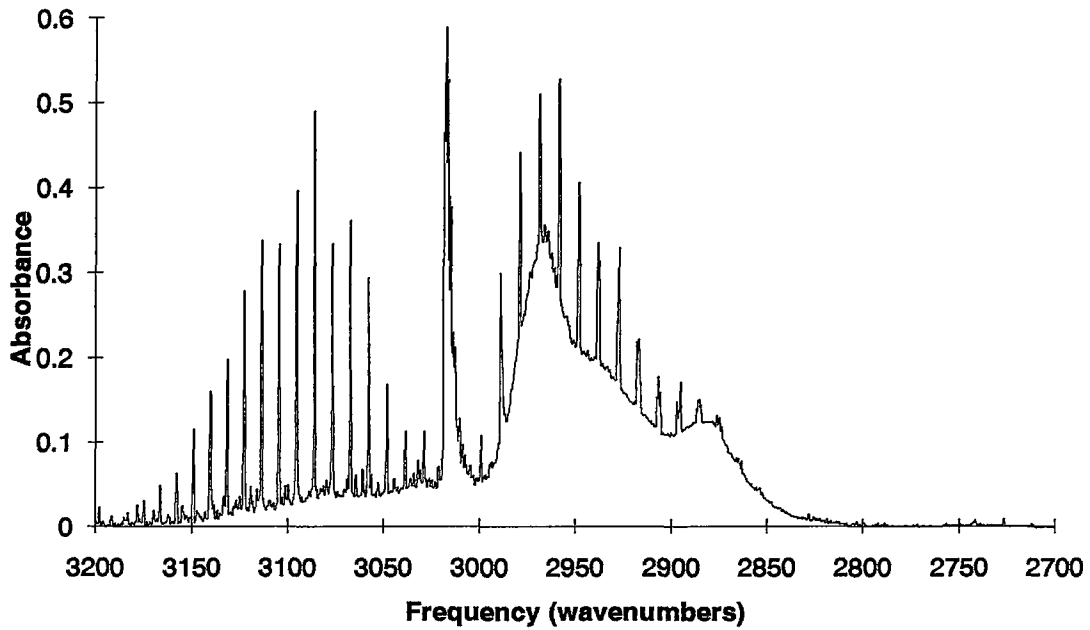


Figure A15. *Spectrum of GM exhaust sample A60301B² with measured HC of 364.6 ppmC.*

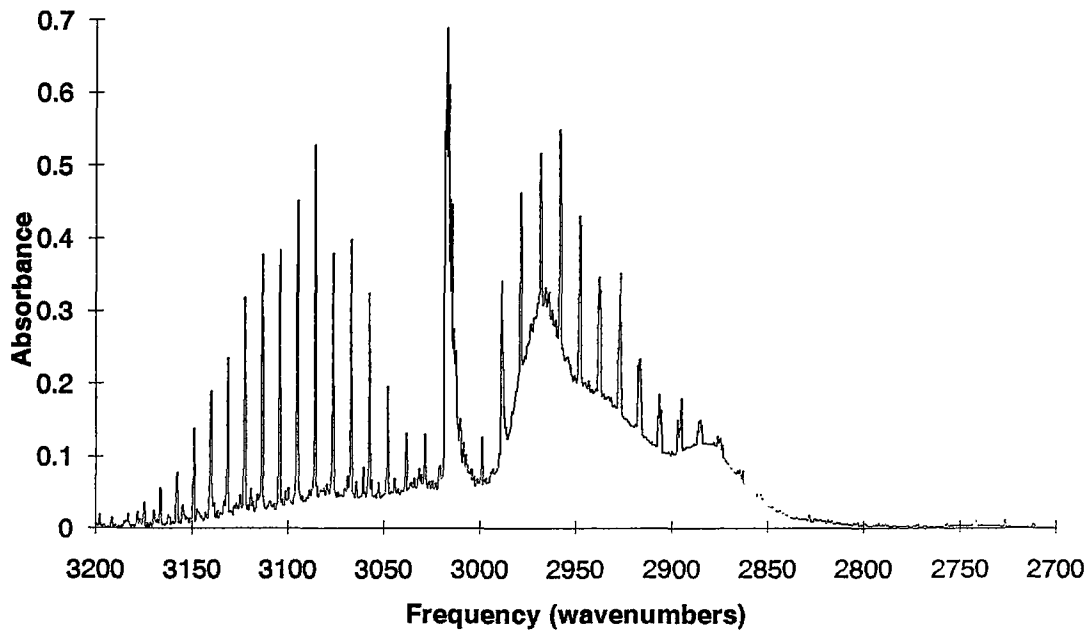


Figure A16. *Spectrum of GM exhaust sample A60401B² with measured HC of 418.9 ppmC.*

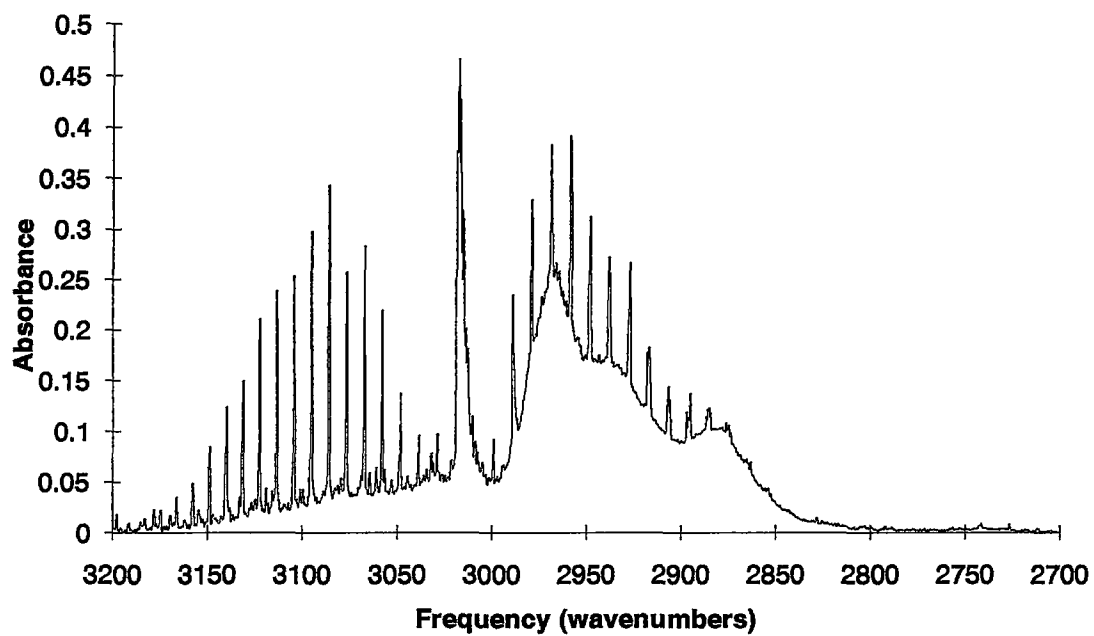


Figure A17. *Spectrum of GM exhaust sample A60901B² with measured HC of 309.9 ppmC.*

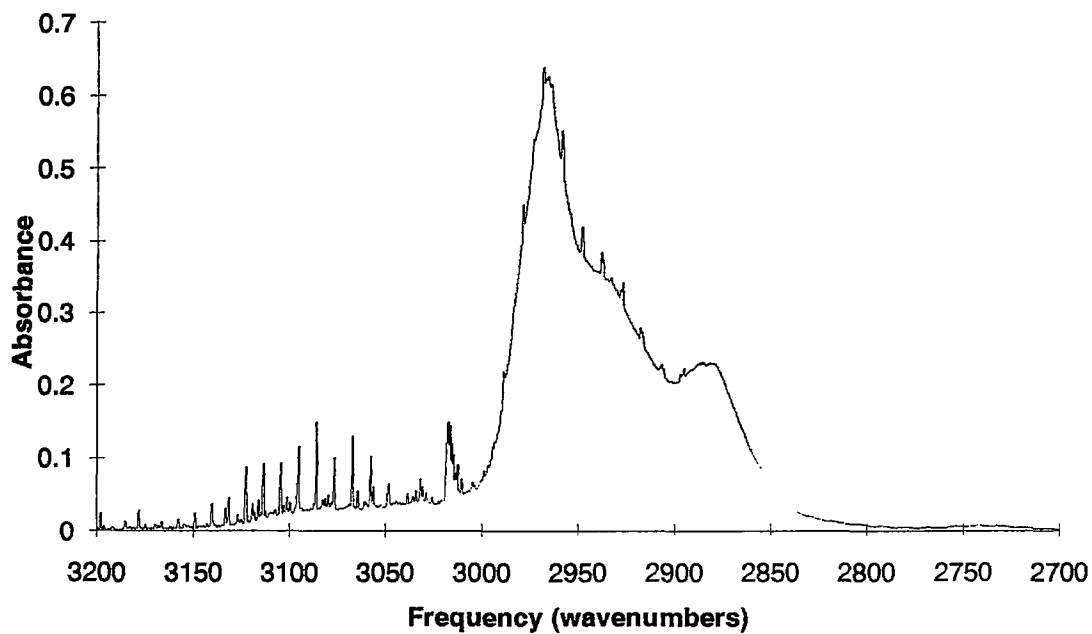


Figure A18. *Spectrum of GM exhaust sample B52701B² with measured HC of 389.1 ppmC.*

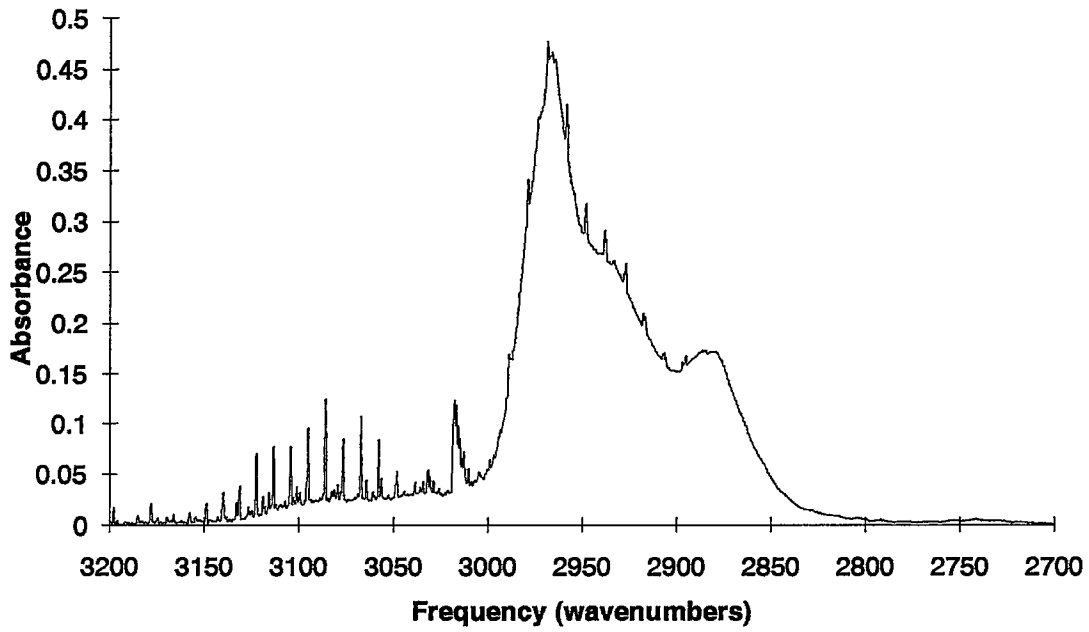


Figure A19. Spectrum of GM exhaust sample B52801A² with measured HC of 316.1 ppmC.

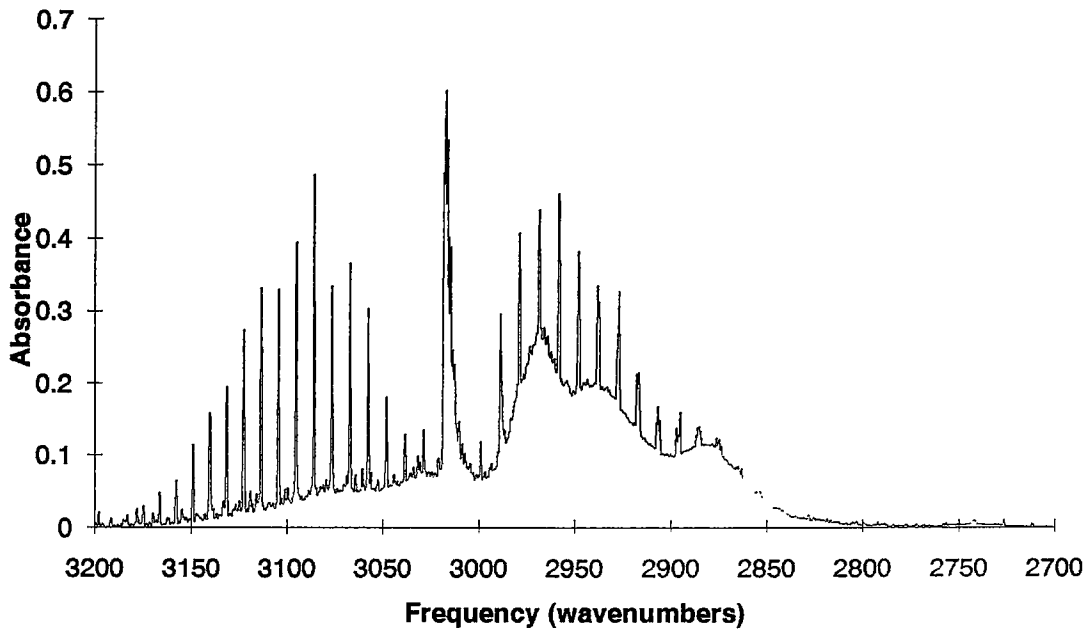


Figure A20. Spectrum of GM exhaust sample B60201B² with measured HC of 402.2 ppmC.

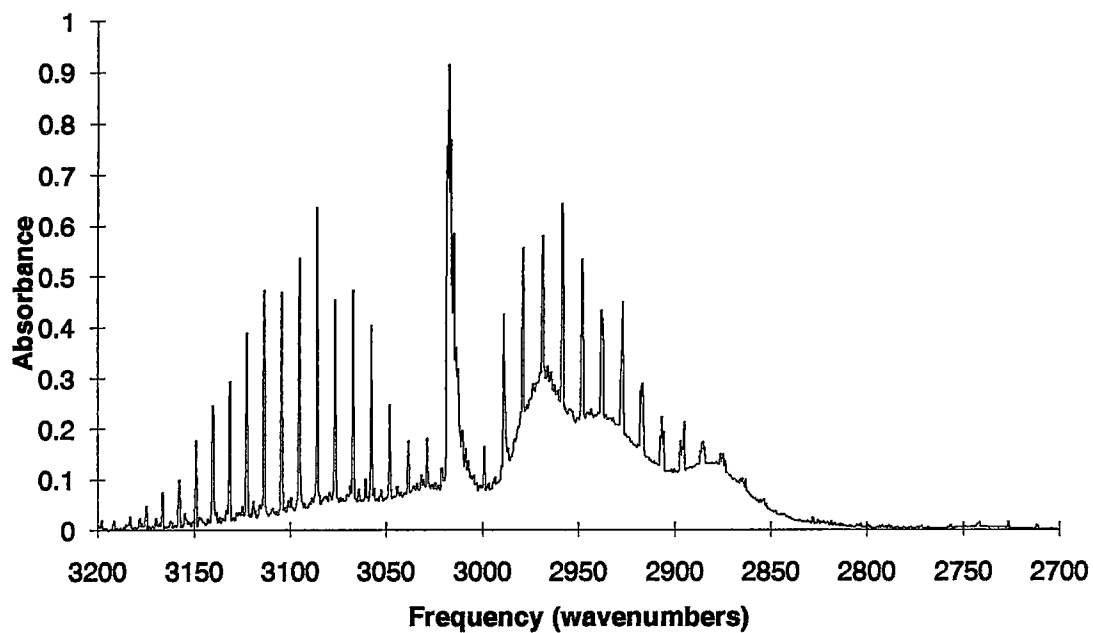


Figure A21. *Spectrum of GM exhaust sample B60202B² with measured HC of 511.3 ppmC.*

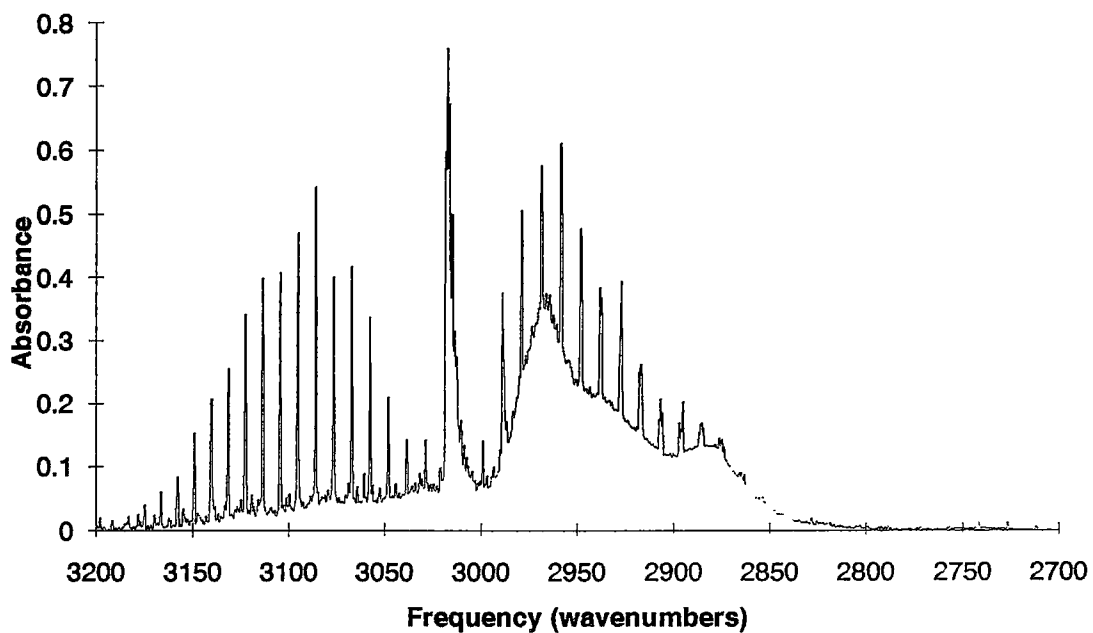


Figure A22. *Spectrum of GM exhaust sample B60402B² with measured HC of 438.6 ppmC.*

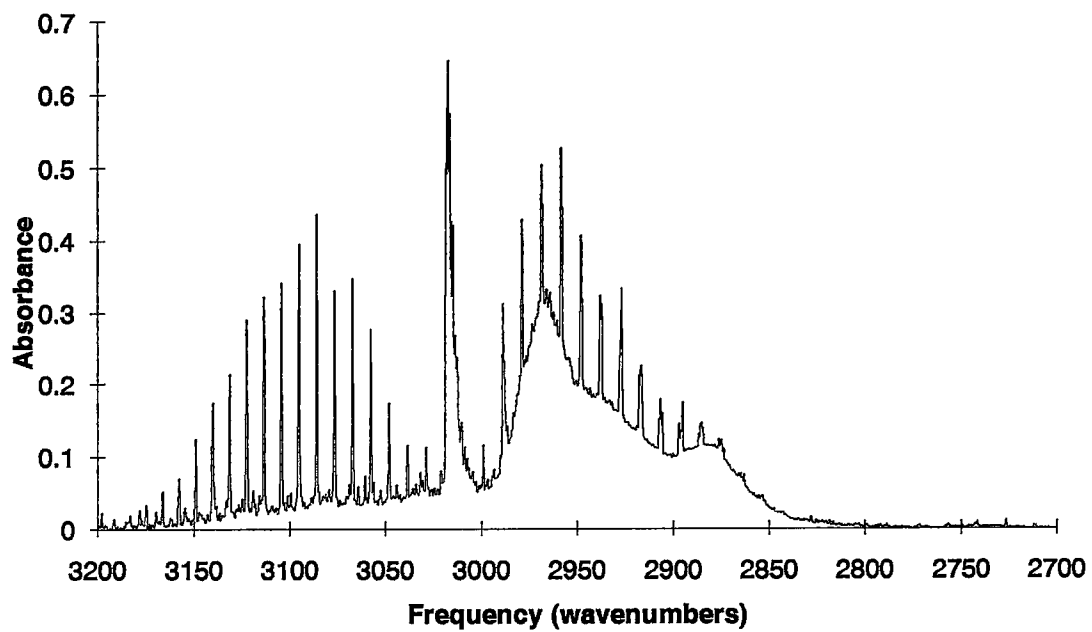


Figure A23. *Spectrum of GM exhaust sample B60701B² with measured HC of 386.1 ppmC.*

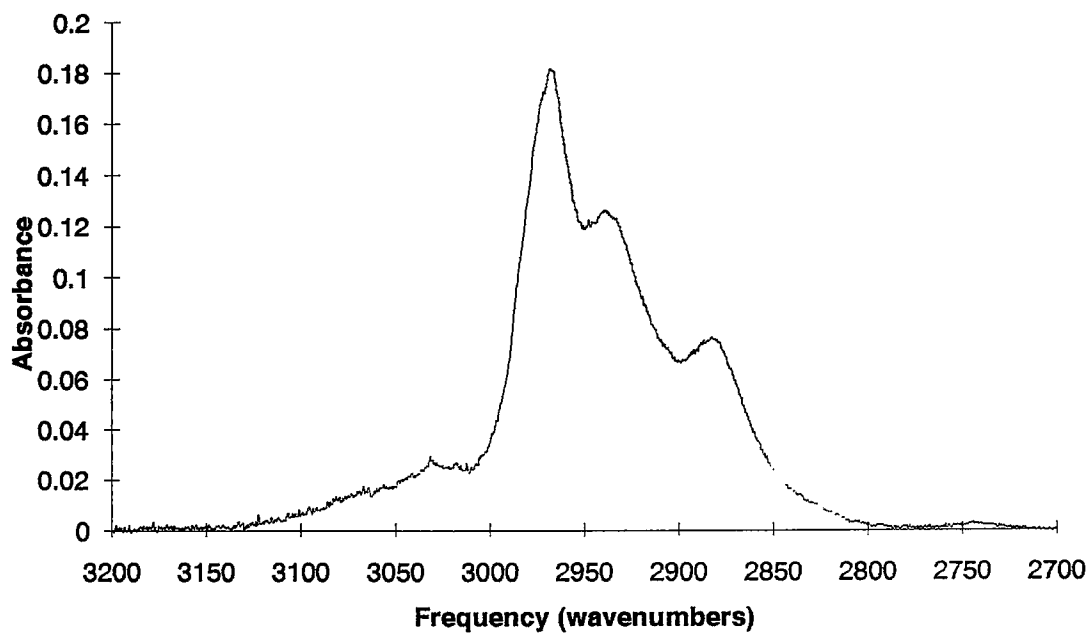


Figure A24. *Spectrum of fuel sample RF18A614T² with measured HC of 141.9 ppmC.*

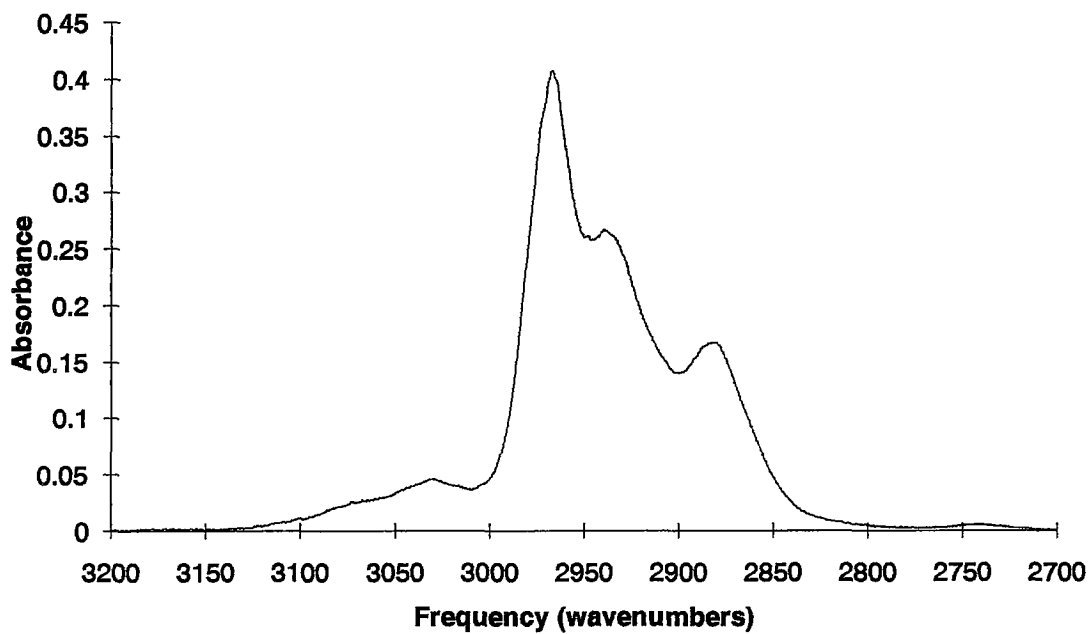


Figure A25. *Spectrum of fuel sample RFA526T² with measured HC of 275.2 ppmC.*

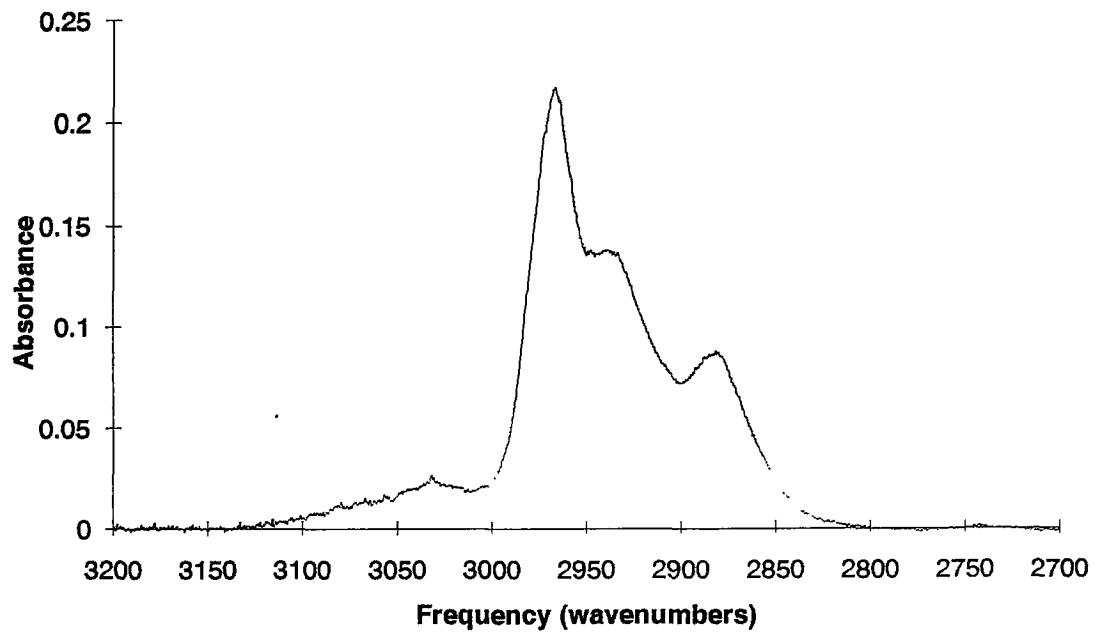


Figure A26. *Spectrum of fuel sample RFA614T² with measured HC of 159.9 ppmC.*

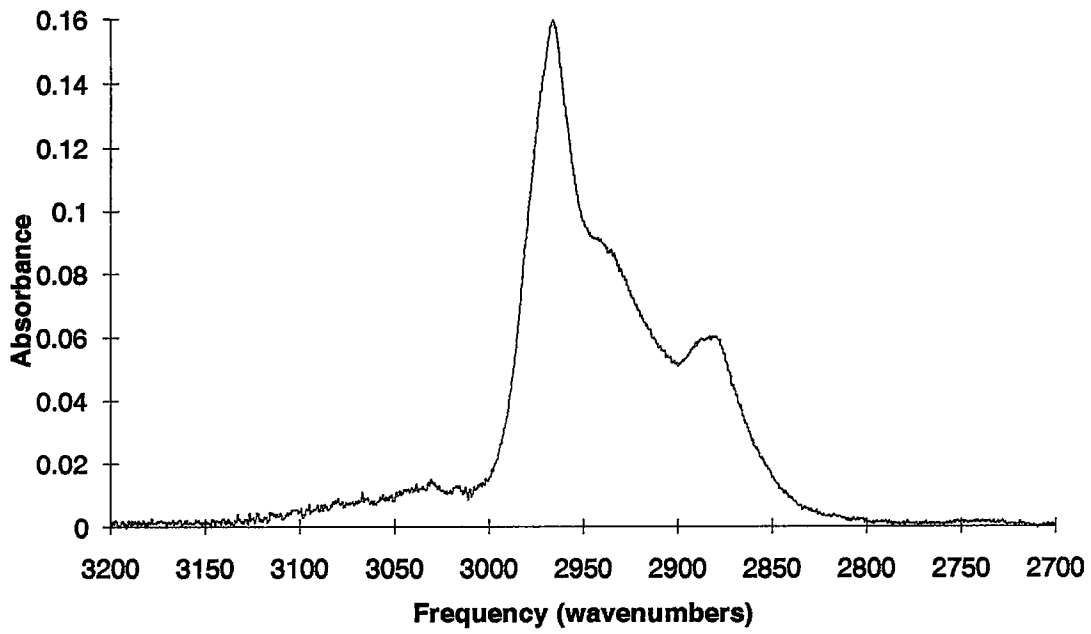


Figure A27. *Spectrum of fuel sample RFF609T² with measured HC of 104.0 ppmC.*

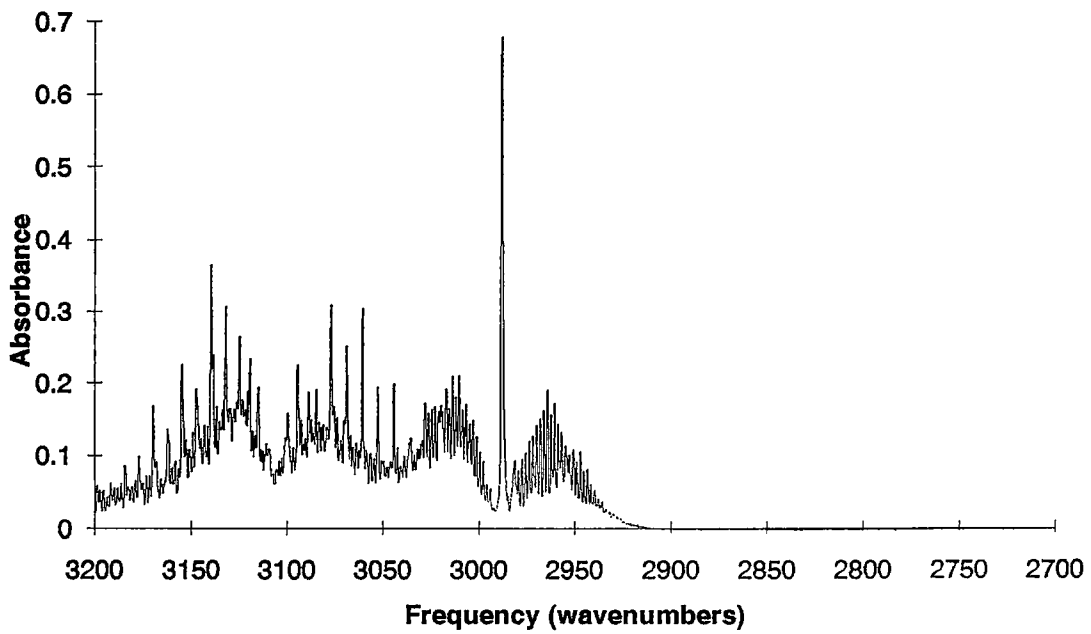


Figure A28. *Spectrum of ethylene sample with measured HC of 648 ppmC.*

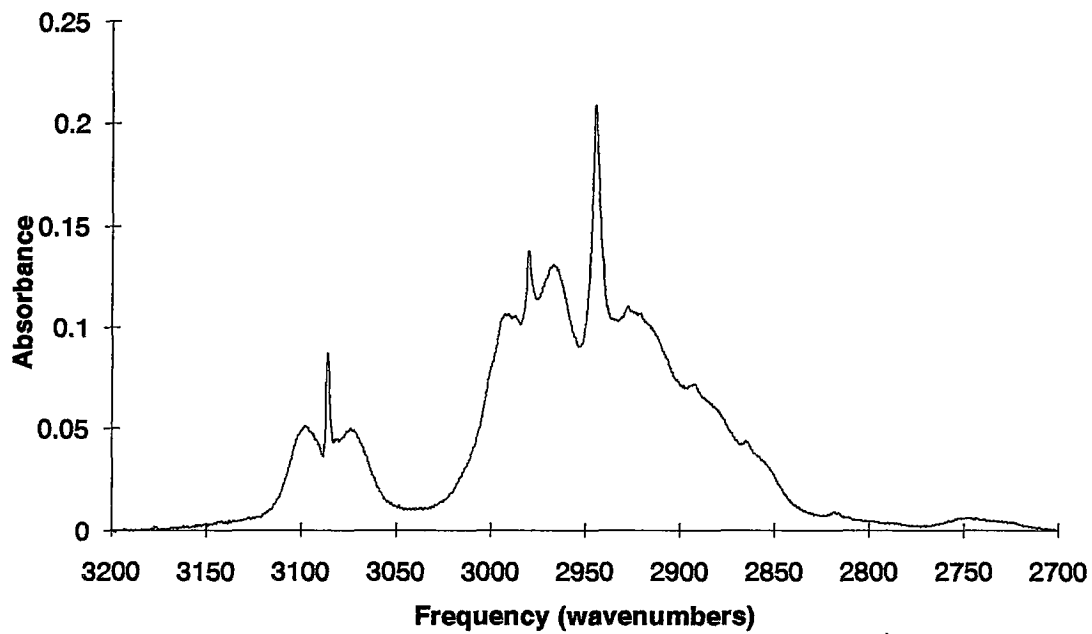


Figure A29. *Spectrum of isobutylene sample with measured HC of 429 ppmC.*

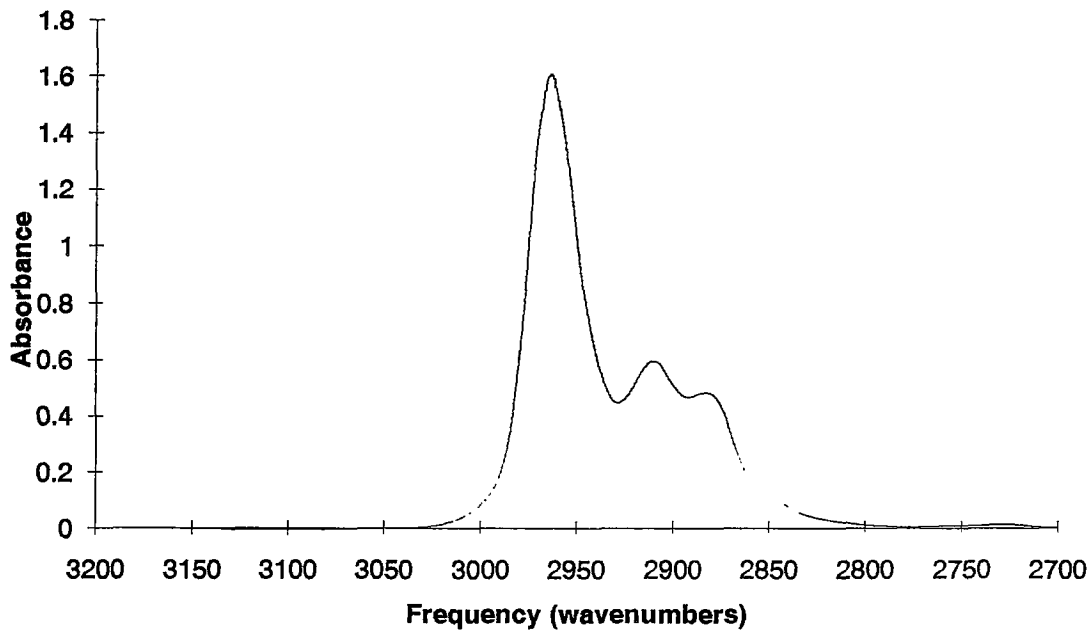


Figure A30. *Spectrum of isooctane sample with measured HC of 720 ppmC.*

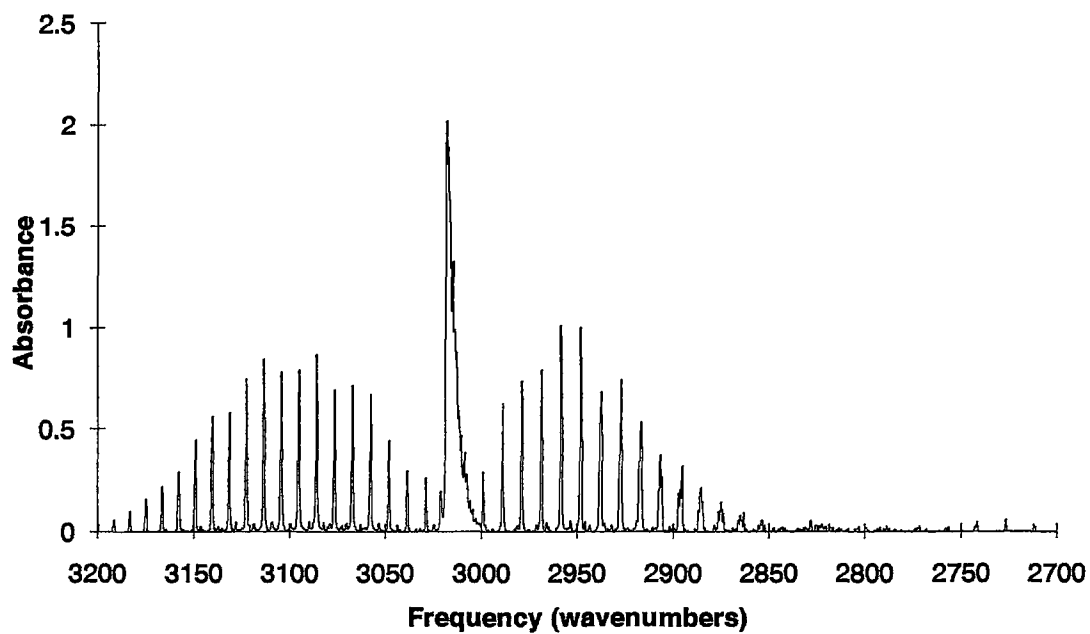


Figure A31. *Spectrum of methane sample with measured HC of 495 ppmC.*

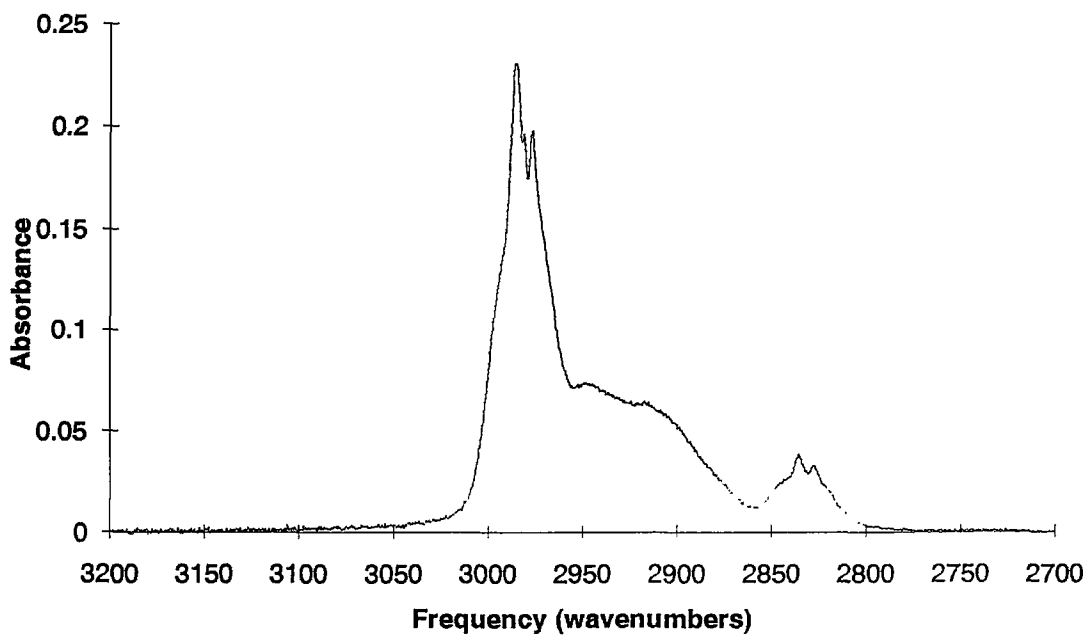


Figure A32. *Spectrum of methyl-t-butyl ether sample with measured HC of 102 ppmC.*

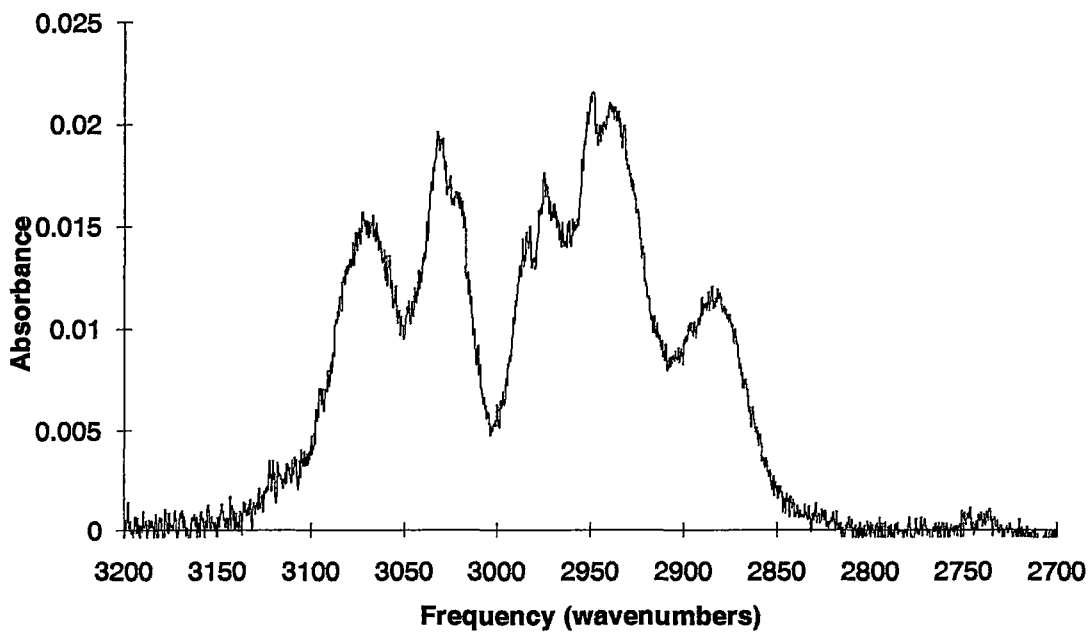


Figure A33. *Spectrum of o-xylene sample with measured HC of 87 ppmC.*

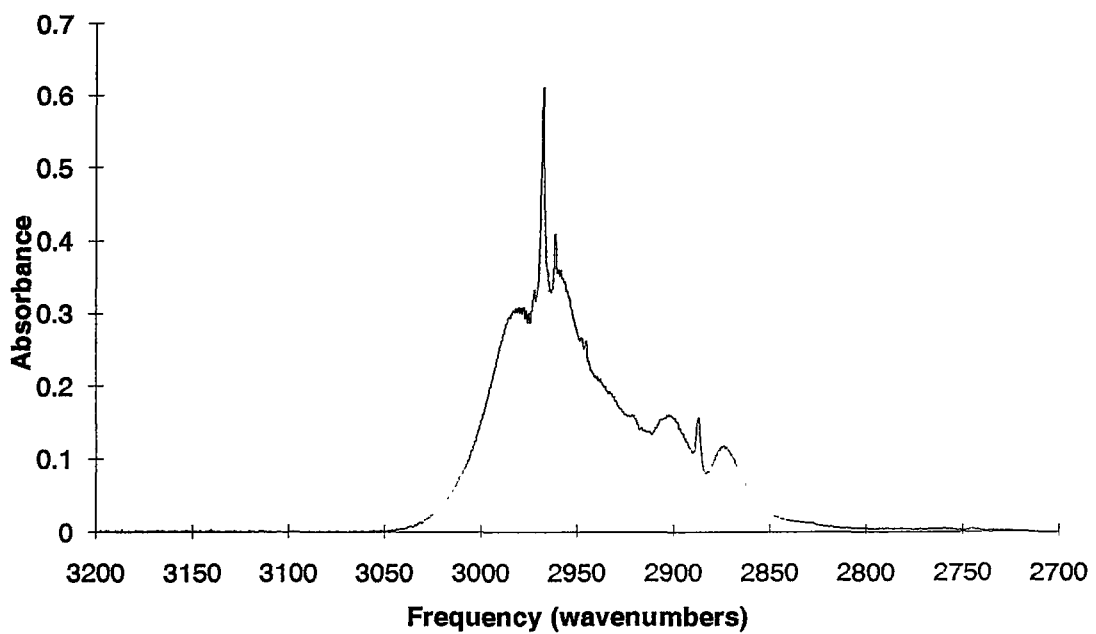


Figure A34. *Spectrum of propane sample with measured HC of 189 ppmC.*

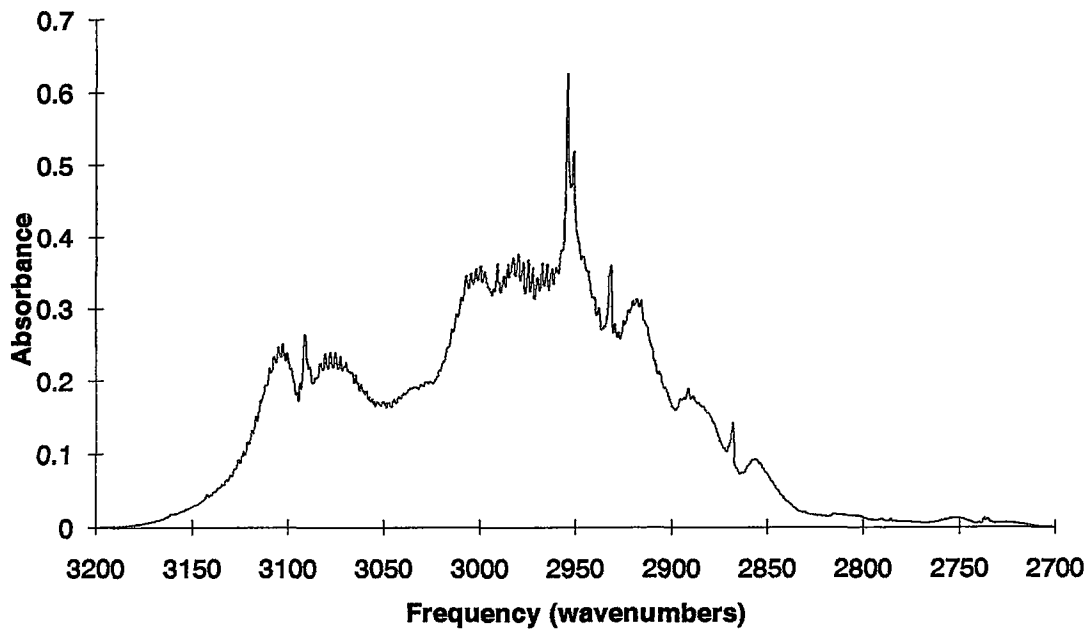


Figure A35. *Spectrum of propene sample with measured HC of 1101 ppmC.*

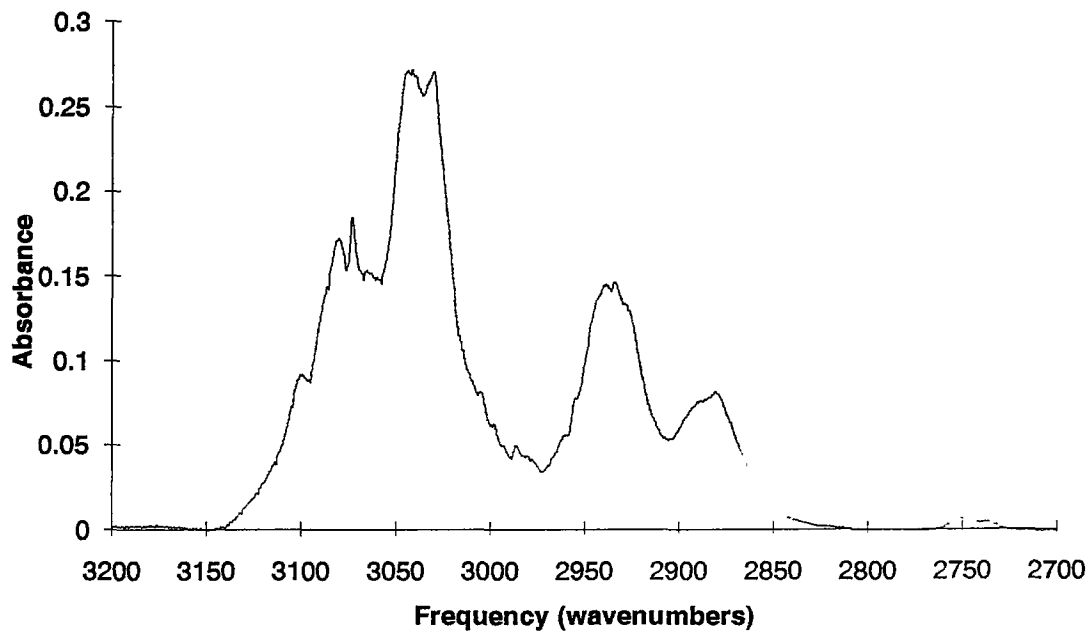


Figure A36. *Spectrum of toluene sample with measured HC of 753 ppmC.*

Distribution List

GM R&D Center

Analytical Chemistry
Dave McEwen
Steve Swarin
Analytic Process
Keki Irani
John Joyce
Consumer and Operations Research
Gary McDonald
Engine Research
Nick Gallopoulos
Instrumentation
Jack Howes
Jay Parikh
Physical Chemistry
Galen Fisher
Steve Harris
Physics
Jeff Sell
Research Technology Partnerships
Kristin Zimmerman

AC Rochester, Milford

Steve Mahan

Environmental and Energy Staff

Bill Watson

Hughes Environmental Systems, Inc.

Nelson Sorbo

Hughes Santa Barbara Research Center

Michael Dahlen
Michael Jack
Dave Nelson

Legal Staff

George Grove
Mark Hester

Powertrain

Harold Haskew
Steve Kornblum